

## **Sentinel-5-Precursor + Innovation**

### **Exploitation of Sentinel-5-p (S5p) for Ocean Colour (S5POC):**

### **S5p diffuse attenuation ( $K_d$ ) product in Sentinel-5-p (S5p) Productive Algorithm Laboratory (PAL)**

### **Validation Report**


**Authors: A. Bracher, S. N. Losa, J. Oelker**

Ref: S5POC-PAL-KD-VR

Version: 1.0

Date: 20-12-2024

For: ESA and S&T

 <p><b>Exploitation of Sentinel-5-P for Ocean Colour Products (S5POC)</b></p>	<p>Validation Report</p>	<p>Ref: S5POC-PAL-VR Version: 1.0 Date: 20-12-2024 For: ESA and S&amp;T</p>
--	--------------------------	---

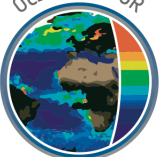


### Change log

Version	Date	Comments	Authors/Organisation
1.0	20-Dec-2024	Final version for PAL	A. Bracher (AWI/IUP)


### Project team

- Astrid Bracher: project leader – AWI.
- Alfredo Joswar Bellido Rosas (from July 2024), Leonardo Alvarado (in 2022): project scientists, AWI.
- Andreas Richter, Vladimir Rozanov (from March 2024), Alexei Rozanov (from March 2024): project scientists - IUP-UB.
- Further contributions based on S5POC VR [RD-6] from former S5POC project team members Svetlana Losa (AW) and Julia Oelker (AWI/IUP).

 <p>Exploitation of Sentinel-5-P for Ocean Colour Products (S5POC)</p>	<p>Validation Report</p>	<p>Ref: S5POC-PAL-VR Version: 1.0 Date: 20-12-2024 For: ESA and S&amp;T</p>
---	--------------------------	---

## Table of Contents

<b>1</b>	<b><u>PURPOSE AND OBJECTIVE</u></b>	<b>4</b>
<b>2</b>	<b><u>STRUCTURE OF THE DOCUMENT</u></b>	<b>4</b>
<b>3</b>	<b><u>REFERENCES, TERMS AND ACRONYMS</u></b>	<b>4</b>
<b>3.1</b>	<b>REFERENCES</b>	<b>4</b>
<b>3.2</b>	<b>TERMS, DEFINITION AND ABBREVIATIONS</b>	<b>9</b>
<b>4</b>	<b><u>PRODUCT REQUIREMENTS</u></b>	<b>12</b>
<b>5</b>	<b><u>REFERENCE MEASUREMENTS</u></b>	<b>12</b>
<b>5.1</b>	<b>GROUND BASED MONITORING NETWORK</b>	<b>12</b>
<b>5.2</b>	<b>SATELLITE MEASUREMENTS</b>	<b>13</b>
<b>5.3</b>	<b>FIELD CAMPAIGNS</b>	<b>14</b>
<b>5.4</b>	<b>MODELLING SUPPORT</b>	<b>14</b>
<b>6</b>	<b><u>VALIDATION APPROACH</u></b>	<b>15</b>
<b>6.1</b>	<b>RECOMMENDATIONS FOR DATA USAGE</b>	<b>16</b>
<b>6.2</b>	<b>STATUS OF VALIDATION</b>	<b>16</b>
<b>6.3</b>	<b>GEOGRAPHICAL PATTERN</b>	<b>24</b>
<b>6.4</b>	<b>BIAS</b>	<b>27</b>
<b>6.5</b>	<b>DISPERSION</b>	<b>29</b>
<b>6.6</b>	<b>SHORT TERM VARIABILITY</b>	<b>33</b>
<b>6.7</b>	<b>DEPENDENCE ON INFLUENCE QUANTITIES</b>	<b>35</b>
<b>7</b>	<b><u>CONCLUSIONS</u></b>	<b>36</b>

 <p><b>Exploitation of Sentinel-5-P for Ocean Colour Products (S5POC)</b></p>	<p>Validation Report</p>	<p>Ref: S5POC-PAL-VR Version: 1.0 Date: 20-12-2024 For: ESA and S&amp;T</p>
--	--------------------------	---

## 1 Purpose and objective

The objective of this document is to describe the validation operations of the novel Sentinel-5 Precursor (S5p) for Ocean Colour (OC) Product of oceanic light attenuation ( $K_d$ ) which is validated given sensitivity analysis performed with coupled atmosphere-ocean Radiative Transfer Model (RTM) and evaluation against independent satellite data products and in-situ observations. The information on the RTM based sensitivity analysis is detailed within [RD3]. The document is maintained during the development phase and the lifetime of the data products. Updates and new versions will be issued in case of changes in the processing chains or for novel validation exercises.

## 2 Structure of the document

This document is structured in 7 sections. Section 1 introduces this document and its objectives. Section 3 lists related references and acronyms. Section 4 provides product requirements. Independent data (satellite and in-situ) used for product validation are described in section 5. Details on the validation results are described in Section 6. Section 7 concludes.

## 3 References, terms and acronyms


### 3.1 References

Baker, K. S. and Smith, R. C. (1982). Bio-optical classification and model of natural waters. *Limnology and Oceanography* 27, 500–509. doi: <https://doi.org/10.4319/lo.1982.27.3.0500>

Bracher A., Vountas M., Dinter T., Burrows J.P., Röttgers R., Peeken I. (2009) Quantitative observation of cyanobacteria and diatoms from space using PhytoDOAS on SCIAMACHY data. *Biogeosciences* 6: 751-764.

Bracher, A. U. and Wiencke, C. (2000). Simulation of the effects of naturally enhanced uv radiation on photosynthesis of antarctic phytoplankton. *Marine Ecology Progress Series* 196, 127–141

Bracher A., Xi H., Dinter T., Mangin A., Strass V. H., von Appen W.-J., Wiegmann S. (2020) High resolution water column phytoplankton composition across the Atlantic Ocean from ship-

 <p><b>Exploitation of Sentinel-5-P for Ocean Colour Products (S5POC)</b></p>	<p>Validation Report</p>	<p>Ref: S5POC-PAL-VR Version: 1.0 Date: 20-12-2024 For: ESA and S&amp;T</p>
--	--------------------------	---

towed vertical undulating radiometry. *Frontiers in Marine Science* 7: 235, <https://doi.org/10.3389/fmars.2020.00235>

Brewin, R.J.W., Sathyendranath, S., Jackson, T., Barlow, R., et al. (2015) Influence of light in the mixed-layer on the parameters of a three-component model of phytoplankton size class. *Remote Sensing of Environment*, 168: 437-450.

Conde, D., Aubriot, L., and Sommaruga, R. (2000). Changes in uv penetration associated with marine intrusions and freshwater discharge in a shallow coastal lagoon of the Southern Atlantic ocean. *Marine Ecology Progress Series* 207, 19–31. Doi:10.3354/meps207019

Dinter T., Rozanov V., Burrows, J. P., Bracher A. (2015) Retrieval of light availability in ocean waters utilizing signatures of vibrational Raman scattering in hyper-spectral satellite measurements. *Ocean Science*, 11: 373-389.


Frouin R. J., Franz B. A., Ibrahim A., Knobelspiesse K., et al. (2019) Atmospheric Correction of Satellite Ocean-Color Imagery During the PACE Era. *Front. Earth Sci.* 7:145.

ESA-OCCCI (2022). Product User Guide for v6.0 Dataset. ESA Ocean Colour Climate Change Initiative (OC\_CCI) Phase 3. Reference D4.2, Issue 6.1, 4 Nov 2022. Download from <https://climate.esa.int/en/projects/ocean-colour/key-documents/>, last accessed on November 18, 2024.

Gomes, A., Bernardo, N., Carmo, A., Rodrigues, T., and Alcantara, E. (2018). Diffuse attenuation coefficient retrieval in cdom dominated inland water with high chlorophyll-a concentrations. *Remote Sensing*, 1063

Højerslev, N. and Aas, E. (1991). A relationship for the penetration of ultraviolet b radiation into the norwegian sea. *Journal of Geophysical Research: Oceans* 96, 17003–17005. doi:<https://doi.org/10.1029/91JC01822>

Johannessen, S. C., Miller, W. L., and Cullen, J. J. (2003). Calculation of uv attenuation and colored dissolved organic matter absorption spectra from measurements of ocean color. *Journal of Geophysical Research: Oceans* 108. doi:10.1029/2000JC000514

 <p><b>Exploitation of Sentinel-5-P for Ocean Colour Products (S5POC)</b></p>	<p>Validation Report</p>	<p>Ref: S5POC-PAL-VR Version: 1.0 Date: 20-12-2024 For: ESA and S&amp;T</p>
--	--------------------------	---

Kahru, M., Elmgreen, R. (2014). Multidecadal time series of satellite-detected accumulations of cyanobacteria in the Baltic Sea. *Biogeosciences* 11, 3619–3633. Doi: 10.5194/bg-11-3619-2014

Lee, Z., Carder, K. L., and Arnone, R. A. (2002). Deriving inherent optical properties from water color: a multiband quasi-analytical algorithm for optically deep waters. *Appl. Opt.* 41, 5755–5772. doi: 10.1364/AO.41.005755.

Lee, Z.-P., Darecki, M., Carder, K. L., Davis, C. O., Stramski, D., and Rhea, W. J. (2005a). Diffuse attenuation coefficient of downwelling irradiance: An evaluation of remote sensing methods. *Journal of Geophysical Research: Oceans* 110, C02017. doi:10.1029/2004JC002573

Lee, Z.-P., Du, K.-P., and Arnone, R. (2005b). A model for the diffuse attenuation coefficient of downwelling irradiance. *Journal of Geophysical Research: Oceans* 110, C02016. doi:10.1029/2004JC002275

Longhurst A. R. (2010) *Ecological Geography of the Sea*. Academic Press.

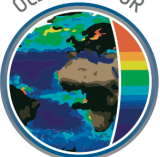
Losa, S. N., Soppa, M. A., Dinter, T., Wolanin, A., Brewin, R. J. W., Bricaud, A., Oelker, J., Peeken, I., Gentili, B., Rozanov, V. V. and Bracher, A. (2017) Synergistic Exploitation of Hyper- and Multi-Spectral Precursor Sentinel Measurements to Determine Phytoplankton Functional Types (SynSenPFT), *Frontiers in Marine Science*, 4 (203), 1-22.

Mason, J. D., Cone, M. T., and Fry, E. S. (2016). Ultraviolet (250–550 nm) absorption spectrum of pure water. *Appl. Opt.* 55, 7163–7172. doi:10.1364/AO.55.007163

Morel, A., Claustre, H., Antoine, D., and Gentili, B. (2007a). Natural variability of bio-optical properties in case 1 waters: attenuation and reflectance within the visible and near-uv spectral domains, as observed in south pacific and mediterranean waters. *Biogeosciences* 4, 913–925. doi:10.5194/bg-4-913-2007

Morel, A., Huot, Y., Gentili, B., Werdell, P. J., Hooker, S. B., and Franz, B. A. (2007b). Examining the consistency of products derived from various ocean color sensors in open ocean (case 1) waters in the perspective of a multi-sensor approach. *Remote Sensing of Environment* 111, 69 – 88. doi:10.1016/j.rse.2007.03.012

Nelson, N. B. and Siegel, D. A. (2002). Chapter 11 - chromophoric dom in the open ocean. In

 <p><b>Exploitation of Sentinel-5-P for Ocean Colour Products (S5POC)</b></p>	<p>Validation Report</p>	<p>Ref: S5POC-PAL-VR Version: 1.0 Date: 20-12-2024 For: ESA and S&amp;T</p>
--	--------------------------	---

Biogeochemistry of Marine Dissolved Organic Matter, eds. D. A. Hansell and C. A. Carlson (San Diego: Academic Press). 547 – 578. doi:10.1016/B978-012323841-2/50013-0

Nicolaus, M., Hudson, S. R., Gerland, S., and Munderloh, K. (2010). A modern concept for autonomous and continuous measurements of spectral albedo and transmittance of sea ice. *Cold Regions Science and Technology* 62, 14 – 28. Doi:10.1016/j.coldregions.2010.03.001

Oelker J. (2021) Suitability of atmospheric satellite sensors for ocean color applications. PhD Thesis, 150 pages, Department of Physics and Engineering, University Bremen, Bremen, Germany, Bremen, 2021. Doi: 10.26092/elib/1100.

Sadeghi A., Dinter T., Vountas M., Taylor B., Peeken I., Soppa M. A., Bracher A. (2012) Improvements to the PhytoDOAS method for identification of coccolithophores using hyperspectral satellite data. *Ocean Science*, 8: 1055-1070.

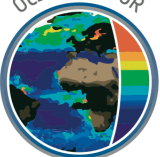
Oelker J., Richter A., Dinter T., Rozanov V. V., Burrows J. P., Bracher A. (2019) Global diffuse attenuation coefficient derived from vibrational Raman scattering detected in hyperspectral backscattered satellite spectra. *Optics Express*, 27 (12): A829-A855.

Oelker J., Losa S. N., Richter A., Bracher A. (2022) TROPOMI-retrieved underwater light attenuation in three spectral regions in the ultraviolet to blue. *Frontiers in Marine Science* 9. 787992. doi: 10.3389/fmars.2022.787992.

Sathyendranath, S., Brewin, R., Brockmann, C., Brotas, V., Calton, B., Chuprin, A., et al. (2019). An ocean-colour time series for use in climate studies: the experience of the ocean-colour climate change initiative (OC-CCI). *Sensors* 19, 4285. doi: 10.3390/s19194285

Sathyendranath, S., Jackson, T., Brockmann, C., Brotas, V., Calton, B., Chuprin, A., et al. (2020). ESA Ocean Colour Climate Change Initiative (ocean\_colour\_cci): Global Chlorophyll-A Data Products Gridded on a Sinusoidal Projection, Version 4.2. Centre for Environmental Data Analysis. Technical report.

Smyth, T. J. (2011). Penetration of uv irradiance into the global ocean. *Journal of Geophysical Research: Oceans* 116. doi:https://doi.org/10.1029/2011JC007183

 <p><b>Exploitation of Sentinel-5-P for Ocean Colour Products (S5POC)</b></p>	<p>Validation Report</p>	<p>Ref: S5POC-PAL-VR Version: 1.0 Date: 20-12-2024 For: ESA and S&amp;T</p>
--	--------------------------	---

Uitz, J., Claustre, H., Morel, A., Hooker, S. B. (2006) Vertical distribution of phytoplankton communities in open ocean: An assessment based on surface chlorophyll. *J. Geophys. Res.*, 111, C08005, doi:10.1029/2005JC003207.

van Geffen, J., Boersma, K. F., Eskes, H., Sneep, M., ter Linden, M., Zara, M., et al. (2020). S5P TROPOMI NO<sub>2</sub> slant column retrieval: method, stability, uncertainties and comparisons with OMI. *Atmospheric Measurement Techniques* 13, 1315–1335. doi:10.5194/amt-13-1315-2020

Vasilkov, A., Krotkov, N., Herman, J., McClain, C., Arrigo, K., and Robinson, W. (2001). Global mapping of underwater uv irradiances and dna-weighted exposures using total ozone mapping spectrometer and sea viewing wide field-of-view sensor data products. *Journal of Geophysical Research* 106, 27205–27219. doi:10.1029/2000JC000373

Vasilkov, A. P., Herman, J. R., Ahmad, Z., Kahru, M., and Mitchell, B. G. (2005). Assessment of the ultraviolet radiation field in ocean waters from space-based measurements and full radiative-transfer calculations. *Appl. Opt.* 44, 2863–2869. doi:10.1364/AO.44.002863

Vernet, M., Brody, E. A., Holm-Hansen, O., and Mitchell, B. G. (1994). The Response of Antarctic Phytoplankton to Ultraviolet Radiation: Absorption, Photosynthesis, and Taxonomic Composition (American Geophysical Union (AGU)). 143–158. doi: 10.1029/AR062p0143


Vodacek, A. and Blough, N. V. (1997). Seasonal variation of CDOM in the Middle Atlantic Bight: terrestrial inputs and photooxidation. In *Ocean Optics XIII*, eds. S. G. Ackleson and R. J. Frouin. International Society for Optics and Photonics (SPIE), vol. 2963, 132 – 137. doi:10.1117/12.266432

Werdell, P. J., Franz, B. A., Bailey, S. W., Harding, L. W. Jr., and Feldman, G. C. (2007). Approach for the long-term spatial and temporal evaluation of ocean color satellite data products in a coastal environment. *Proc. SPIE* 6680:66800G. doi: 10.1117/12.732489

[RD1] Soppa M. A., Losa S. N., Oelker J., Brotas V., Costa M., Rio M.-H., Sa C., Bracher A. (2019) Sentinel-5P Ocean Color: Requirements Baseline Document. S5POC-RBD-D01 v1.0. [https://www.awi.de/fileadmin/user\\_upload/AWI/Forschung/Klimawissenschaft/Physikalische\\_Ozeanographie\\_der\\_Polarmeere/Download/S5POC-RB-D01\\_v1.0.pdf](https://www.awi.de/fileadmin/user_upload/AWI/Forschung/Klimawissenschaft/Physikalische_Ozeanographie_der_Polarmeere/Download/S5POC-RB-D01_v1.0.pdf)

[RD2] Losa S. N., Brotas V., Brito A., Costa M., Dinter T., Favareto L., Gomes M., Oelker J., Rio



 <p><b>Exploitation of Sentinel-5-P for Ocean Colour Products (S5POC)</b></p>	<p>Validation Report</p>	<p>Ref: S5POC-PAL-VR Version: 1.0 Date: 20-12-2024 For: ESA and S&amp;T</p>
--	--------------------------	---

M.-H., Sa C., Soppa M.S., Suseelan V. P., Bracher A. (2022) Sentinel-5P Ocean Colour: Data Pool and Auxiliary User Manual 2 (DP + AUM2; S5POC\_DP-D2\_AUM2-D8). Version 1.2, 13 May 2022.

[https://www.awi.de/fileadmin/user\\_upload/AWI/Forschung/Klimawissenschaft/Physikalische\\_Ozeanographie\\_der\\_Polarmeere/S5POC\\_DP-D02\\_AUM2-D08\\_v1.2\\_13052022\\_signed.pdf](https://www.awi.de/fileadmin/user_upload/AWI/Forschung/Klimawissenschaft/Physikalische_Ozeanographie_der_Polarmeere/S5POC_DP-D02_AUM2-D08_v1.2_13052022_signed.pdf)

[RD3] Bracher A., Oelker J., Bellido Rosas A. J., Richter A. (2024) Exploitation of Sentinel-5-p (S5p) for Ocean Colour Products (S5POC) - S5p diffuse attenuation ( $K_d$ ) product in Sentinel-5-p (S5p) Productive Algorithm Laboratory (PAL): Algorithm Theoretical Base Document (S5POC-PAL-KD-ATBD) Version 1.0, 20 Dec 2024, S5POC\_PAL\_KD\_ATBD\_v1.0\_20122024.pdf


[RD4] Bracher A., Bellido Rosas A. J. (2024) Exploitation of Sentinel-5-p (S5p) for Ocean Colour Products (S5POC) -Diffuse attenuation ( $K_d$ ) product in Sentinel-5-p (S5p) Productive Algorithm Laboratory (PAL): Product User Manual (S5POC-PAL-KD-PUM). Version 1.0, 23 Dec 2024, S5POC\_PAL\_KD\_PUM\_v1.0\_23122024.pdf

[RD5] Bracher A., Alvarado A., Richter A., Rio M.-H., Brotas V., Brito A., Costa M. (2022a) Sentinel-5P Ocean Colour: Impact Assessment Report. S5POC-IAR-D9 Version 1.1, 13 May 2022. S5POC\_IAR-D9\_v1.1\_13052022.pdf, [https://www.awi.de/fileadmin/user\\_upload/AWI/Forschung/Klimawissenschaft/Physikalische\\_Ozeanographie\\_der\\_Polarmeere/S5POC-IAR-D9\\_v1.1\\_13052022-signed.pdf](https://www.awi.de/fileadmin/user_upload/AWI/Forschung/Klimawissenschaft/Physikalische_Ozeanographie_der_Polarmeere/S5POC-IAR-D9_v1.1_13052022-signed.pdf)

[RD6] Bracher, A., Losa, S., Brotas, V., Oelker, J., Rio, M.-H., & Xi, H. (2022b) Sentinel-5P Ocean Colour: Validation Report. S5POC VR Version 3.1. 13 May 2022. Tech. rept. Alfred Wegener Institute (AWI), Helmholtz Centre for Polar and Marine Research; Institute of Environmental Physics, University of Bremen; Faculdade de Ciencias, Universidade de Lisboa. S5POC\_VR-D5\_v3.1\_13052022.pdf


### 3.2 Terms, definition and abbreviations

- AUM ----- Auxiliary Dataset User Manual
- AWI ----- Alfred Wegener Institute Helmholtz Centre for Polar and Marine Research
- CCD ----- Charge-coupled Device
- CDOM ----- Coloured Organic Dissolved Matter
- CHL ----- Chlorophyll-a concentration

 <p><b>Exploitation of Sentinel-5-P for Ocean Colour Products (S5POC)</b></p>	<p>Validation Report</p>	<p>Ref: S5POC-PAL-VR Version: 1.0 Date: 20-12-2024 For: ESA and S&amp;T</p>
--	--------------------------	---

CMEMS ----- Copernicus Marine Environmental Services  
 CSA ----- Canadian Space Agency  
 D ----- Deliverable  
 DKRZ ----- German Climate Computing Center  
 DOAS ----- Differential Optical Absorption Spectroscopy  
 DP ----- Data Pool  
 ENVISAT ----- Environmental Satellite  
 ESA ----- European Space Agency  
 FC.ID ----- Associação para a Investigação e Desenvolvimento de Ciências  
 GOME ----- Global Ozone Monitoring Experiment  
 HPLC ----- High-Performance Liquid Chromatography  
 IA ----- Impact Assessment  
 IOP ----- Inherent optical properties  
 IUP ----- Institute of Environmental Physics, University of Bremen  
 Kd ----- Diffuse attenuation coefficient  
 KD490 ----- Diffuse attenuation coefficient at 490 nm  
 KD490 ----- Operational Kd490 product from S3-OLCI and OCCCI  
 Kdblue ----- Diffuse attenuation coefficient from 390 nm to 423 nm  
 KdUVA ----- Diffuse attenuation coefficient from 356.5 nm to 390 nm  
 KdUVAB ----- Diffuse attenuation coefficient from 312.5 nm to 338.5 nm  
 LUT ----- Look Up Table  
 MERIS ----- Medium Resolution Imaging Spectrometer  
 MODIS ----- Moderate-resolution Imaging Spectroradiometer  
 OC ----- Ocean Colour  
 OCCCI ----- Ocean Colour Climate Change Initiative  
 OLCI ----- Ocean and Land Colour Instrument  
 OMI ----- Ozone Monitoring Instrument  
 PAL ----- Production Algorithm Laboratory  
 PFT ----- Phytoplankton Functional Type  
 PP ----- Prototype Products  
 PUM ----- Product User Manual  
 RB ----- Requirements Baseline  
 RRS ----- Remote Sensing Reflectance  
 RTM ----- Radiative Transfer Model  
 RV ----- Research Vessel  
 S3 ----- Sentinel-3



 <p><b>Exploitation of Sentinel-5-P for Ocean Colour Products (S5POC)</b></p>	<p>Validation Report</p>	<p>Ref: S5POC-PAL-VR Version: 1.0 Date: 20-12-2024 For: ESA and S&amp;T</p>
--	--------------------------	---

## 4 Product requirements


Details on product requirements can be found in [RD1], section 7. The developed S5POC retrievals of diffuse attenuation coefficients ( $K_d$ ) for TROPOMI (on S5p) are based on Differential Optical Absorption Spectroscopy (DOAS) in combination with radiative transfer modelling (RTM), [RD3]. As input information the algorithm requires RTM simulated reference spectra (RRS, VRS, ocean weighting function), measured reference absorption spectra (water, atmospheric trace gases) and TROPOMI and RTM simulated L1 (top of atmosphere, TOA) radiance and extra-terrestrial irradiance data. Overall, the scientific (section 7.1 in [RD1]) w.r.t. spatial, temporal, spectral and radiometric resolution can be met in general with the TROPOMI instrument settings. However, because of different and less wavelength range the PhytoDOAS algorithms and products developed are specifically adapted to match TROPOMI settings for wavelength coverage (see sections 4.4.2 in [RD3] on fit window settings for the three  $K_d$  products). TROPOMI has different and non-beneficial instrumental UV-VIS setting as compared to SCIAMACHY, which are that no data are acquired at 500-675 nm and its spectral resolution is lower with  $\sim 1$  nm as opposed to 0.4 nm in the UV-VIS (see also risk analysis given in section 6 of [RD1]). It is worth mentioning that TROPOMI has lower signal-to-noise ratio (SNR) than Sentinel-3 OLCI (at  $\sim 500$  nm about 1000 opposed to  $>1500$ ) that could limit retrievals in very dark waters as oceanic gyres or high CDOM waters due to very low water leaving radiance values (Frouin et al. 2019). Operational requirements for global processing of  $K_d$  products for global can be met by the S5p Production Algorithm Laboratory (PAL).

## 5 Reference measurements

The developed S5POC TROPOMI  $K_d$  products are evaluated given available multispectral satellite products and *in-situ* datasets as presented in the following subsections.

### 5.1 Ground based monitoring network

The S5POC  $K_d$  products are validated for four selected test regions: Atlantic Ocean (separated into temperate and tropical vs. high Northern latitude waters (Regions C and D, Figure 1). For these areas there are a number of *in-situ* measurements from a series of field campaign and surveys of AWI (for details see [RD1, RD2]). For ocean color validation concerning the products developed within S5POC no ground-based network data were available for the time May 2018 until end of 2020 until the time the data base was finally submitted (6 July 2022, [RD2]).

 <p><b>Exploitation of Sentinel-5-P for Ocean Colour Products (S5POC)</b></p>	<p>Validation Report</p>	<p>Ref: S5POC-PAL-VR Version: 1.0 Date: 20-12-2024 For: ESA and S&amp;T</p>
--	--------------------------	---

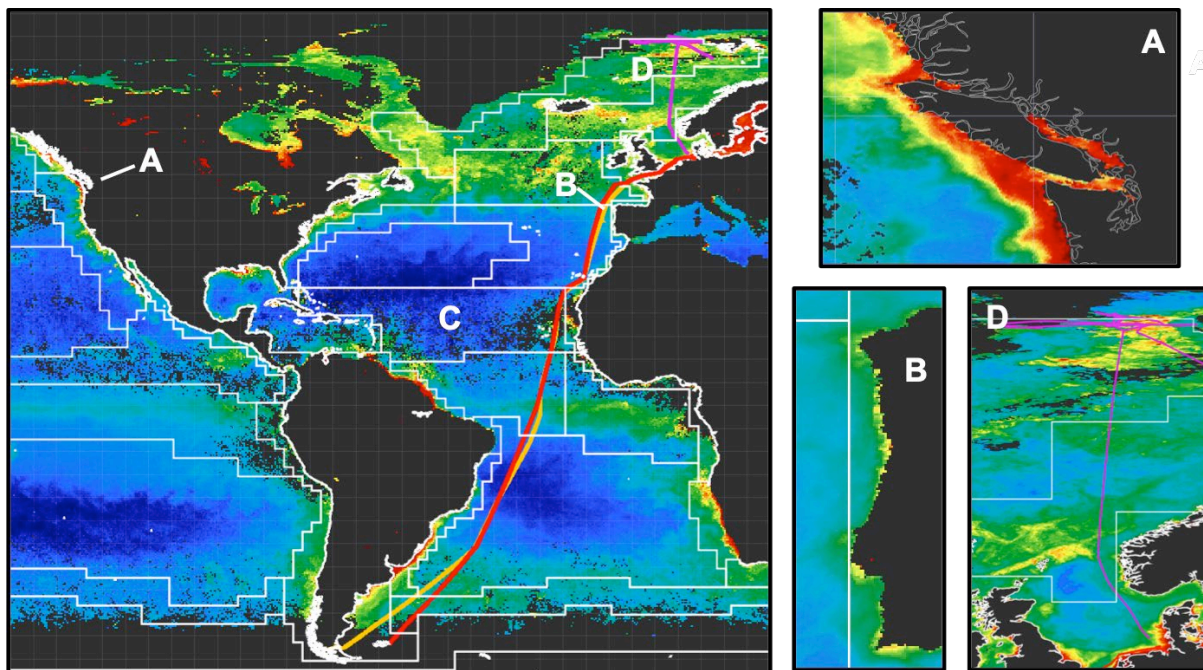



Figure 1: Test regions used to develop S5POC products: A-Salish Sea (no  $K_d$  data), B-Portugal's Atlantic Coast (no  $K_d$  data), C Transatlantic Ocean and D Northern-Atlantic Ocean. The colors represent chlorophyll a concentration (CHL in  $\text{mg}/\text{m}^3$ ) in July 2019 (ESA OCCCI, <https://esa-oceancolour-cci.org/>); waters with low CHL appear in blue colors and higher CHL in yellow and red colors. The white lines are the limits of the Longhurst biogeochemical provinces (Longhurst, 2010). Research Vessel (RV) Polarstern PS113, PS120 and PS121 cruise tracks are plotted in orange, red and purple, respectively. These are the expeditions where in-situ  $K_d$  data were available.

## 5.2 Satellite measurements

The developed S5POC TROPOMI  $K_d$  data products are compared against similar products obtained with Level 2 of OLCI (on Sentinel-3A and -3B) KD490 (diffuse attenuation at 490 nm) data at full resolution (300 m) provided as Near Real-Time product [RD2]. This operational KD490 product is calculated based on the OK2-560 algorithm (Morel et al., 2007b) which is based on an empirical relation between Chlorophyll-a concentration (Chla) and KD490, with Chla derived from an empirical band-ratio algorithm. OLCI data was downloaded via EUMETSAT Streaming Service (version IPF 6.11, processing baseline v2.23). As second multispectral data set, the OC-CCI data set (Sathyendranath et al., 2019) version 4.2 (Sathyendranath et al., 2020) (<http://www.esa-oceancolour-cci.org>) was used. It is a merged product consisting of information from the MODIS-Aqua and VIIRS sensors for 2018. Data is provided on a sinusoidal grid with 4 km spatial and daily temporal resolution. KD490 is retrieved semi-analytically (Lee et al., 2005b). Absorption and backscattering are first obtained in a quasi-analytical approach (Lee et al., 2002) and then related to KD490 using look-up tables (LUTs) established with radiative transfer modelling. Note that there are no similar OC products derived from other hyperspectral sensors for intercomparison. For this reason, OC products from multispectral sensors are used. Table 1 summarizes information on these

 <p><b>Exploitation of Sentinel-5-P for Ocean Colour Products (S5POC)</b></p>	<p>Validation Report</p>	<p>Ref: S5POC-PAL-VR Version: 1.0 Date: 20-12-2024 For: ESA and S&amp;T</p>
--	--------------------------	---

independent satellite data products and their spatial and temporal resolution. Derived  $K_d$  products from TROPOMI were compared to

Table 1: Satellite datasets for test regions.

Satellite/Data set	Sensor	Processing level	Product	Spatial resolution	Temporal resolution	Period
S3A and S3B	OLCI	1/2	KD490	300 m	daily	2018 - 2020
OCCCI v4.2	Merged	3	KD490 (for 2020 only v5.0 was available), CHL	4 km	daily	2018-2020

### 5.3 Field campaigns


Table 2 summarizes information on the *in-situ* observations collected from 2018 to 2020 in the open Atlantic Ocean (test regions C, D) during several cruises (PS113, PS121, MSM93). Figure 1 shows the test regions maps. The derived *in-situ* spectral  $K_d$  data are used for the S5POC TROPOMI product validation. Detailed information on the campaigns, measurements and the instruments and methods is provided in [RD2].

Table 2: In-situ observations used for S5POC TROPOMI  $K_d$  evaluation.

Observation name	Observation description	Associated measurement	Cruises/survey	Test region
Spectral $K_d$	Light attenuation spectral	Spectral $K_d$	PS113; PS121, MSM93	C D

### 5.4 Modelling support

Modelling is only indirectly used within this project for validation. The project uses the fully-coupled atmosphere-ocean RTM SCIATRAN to derive pseudo-absorption spectra for fitting Rotational Raman Scattering and vibrational Raman scattering (VRS) in the UVA, short blue and blue which are then used within the respective DOAS retrievals. RTM SCIATRAN is further used to derive the conversion of the fit factors of VRS, obtained with DOAS, into physical quantities such as the  $K_d$  at specific wavelength regions (UVAB, UVA and short blue). The conversions are derived via first forward modelling from a set of oceanic and atmospheric conditions and then using the simulated TOA radiances via the DOAS retrieval to derive the VRS-fit results. The RTM is also used to perform complex retrievals' sensitivity analyses. With both finally correction schemes are developed which are then implemented into LUTs (e.g., which further account for the observation geometry, broadband phenomena and separating correlating spectral effects). More details can be found in [RD3].

 <p><b>Exploitation of Sentinel-5-P for Ocean Colour Products (S5POC)</b></p>	<p>Validation Report</p>	<p>Ref: S5POC-PAL-VR Version: 1.0 Date: 20-12-2024 For: ESA and S&amp;T</p>
--	--------------------------	---

## 6 Validation approach

Table 2: Geolocations and time periods of S5POC TROPOMI  $K_d$  products. The time period reflects the time satellite data have been processed to cover the month the specific expedition/survey took place.


Time period	Geolocation	S5POC product	Related expedition/survey	Test region
11 May-10 Jun 2018	50.5°S-52°N, 65°W-12.5°E	$K_d$	PS113	C
11 Aug-10 Sep 2019 25 Jun-24 Jul 2020	55°N-80°N, 25°W-15°E	$K_d$	PS121 MSM93	D

The three spectral range  $K_d$  are determined from S5p TROPOMI data by applying the RTM based LUTs on the VRS fit factors retrieved via the DOAS retrieval for regions C and D and specific time periods as specified in Table 2.  $K_d$  is derived in three spectral regions (Figure 2a): in the short blue from 390 nm to 423 nm (blue), in the UV-A from 356.5 nm to 390 nm (UVA), and in the UV-B to UV-A from 312.5 nm to 338.5 nm (UVAB). RTM settings follow Oelker et al. (2019), but are further adapted to TROPOMI. The results presented here are part of the publication in *Frontiers in Marine Science* (Oelker et al. 2022) and the PhD thesis by Oelker (2021).

Validation of the S5POC TROPOMI  $K_d$  retrievals is performed by intercomparison to *in-situ* measurements and to similar satellite products from multispectral ocean colour sensors. Coupled atmosphere-ocean RTM is used for sensitivity studies. These are mostly detailed in [RD3] and within this document only the main outcome and conclusions are given. The S5POC TROPOMI retrievals for  $K_d$  are retrieved for regions C and D, for monthly time periods covering the time periods of the corresponding campaigns (Table 2).

The match-up statistics are quantified by the metrics described in the OCCCI Product User Guide (ESA-OCCCI 2022). The metrics includes RMSD, un-biased RMSD, bias, slope, intercept (type II regression) and Pearson coefficient of determination. In addition, the mean absolute deviation (MAE) is quantified. Details on the metrics computations are given in section 7.1 of [RD3].

The three spectral range  $K_d$  are determined by applying the RTM based LUTs on the VRS fit factors retrieved via the DOAS retrieval from S5p TROPOMI data for regions C and D and specific time periods as specified in Table 2.  $K_d$  is derived in three spectral regions (Figure 2a): in the short blue from 390 nm to 423 nm (blue), in the UV-A from 356.5 nm to 390 nm (UVA),

 <p><b>Exploitation of Sentinel-5-P for Ocean Colour Products (S5POC)</b></p>	<p>Validation Report</p>	<p>Ref: S5POC-PAL-VR Version: 1.0 Date: 20-12-2024 For: ESA and S&amp;T</p>
--	--------------------------	---

and in the UV-B to UV-A from 312.5 nm to 338.5 nm (UVAB). RTM settings follow Oelker et al. (2019), but are further adapted to TROPOMI. The results presented here are part of the publication in *Frontiers in Marine Science* (Oelker et al. 2022) and the PhD thesis by Oelker (2021).

### 6.1 Recommendations for data usage

All TROPOMI ground pixels are processed within a given region. The S5POC TROPOMI  $K_d$  L2 product contains information on cloud coverage (provided as cloud fraction), ice and land flags provide flags to be used for filtering for valid ground pixels, i.e., land pixels and ice- and cloud-covered pixels should be removed. When a region does not contain any ice covered ocean areas, the snow-ice flag can be ignored and only first the land flag should be used to remove land and inland water pixels. The snow-ice mask also enables a screening of coastal pixels. For cloud screening only S5POC TROPOMI  $K_d$  products with cloud fraction below  $< 0.01$  should be considered. Overall, the S5POC TROPOMI  $K_d$  product quality decreases for highly attenuating ocean scenes. Generally, the product should only be used for open ocean scenes. For more details see [RD3], [RD4], [RD5].

### 6.2 Status of Validation

This section presents a summary of the validation results based on matchups with *in-situ* and satellite data. Validation of S5POC TROPOMI  $K_d$  products (Figure 2) is performed for regions C and D. Results for the Atlantic Ocean over the period of PS113 are detailed in Oelker et al. (2022). S5POC  $K_d$  products are compared to hyperspectral RAMSES data collected *in-situ* for region C during PS113 (11 May – 9 June 2018), both, during discrete stations ( $n=19$ ) and during Triaxus casts ( $n=155$ ), for region D only during stations for PS121 (11 Aug-10 Sep 2019,  $n=17$ ) and only during Triaxus casts for MSM93 (27 Jun to 25 Jul 2020). Since operation of the RAMSES sensor on the towed undulating platform Triaxus (see Bracher et al. 2020) is performed with profiling at a high speed ( $\sim 1\text{m/s}$ ) under the low light conditions in region D (Arctic) no valid *in-situ*  $K_d$  values within the UVAB spectral range could be obtained and also for  $K_d$ -UVA data the number of valid *in-situ* points ( $n=276$ ) was less than for  $K_d$ -blue ( $n=307$ ), see Figure 4. KD490 products from Sentinel-3A full resolution (S3A-FR) and OCCCI available for the same periods. To convert S3A and OCCCI KD490 data to the blue range of S5POC TROPOMI  $K_d$ -blue, or *vice versa* the S5POC TROPOMI  $K_d$ -blue to KD490 we use a conversion function derived from *in-situ* RAMSES data (Figure 2b, c).



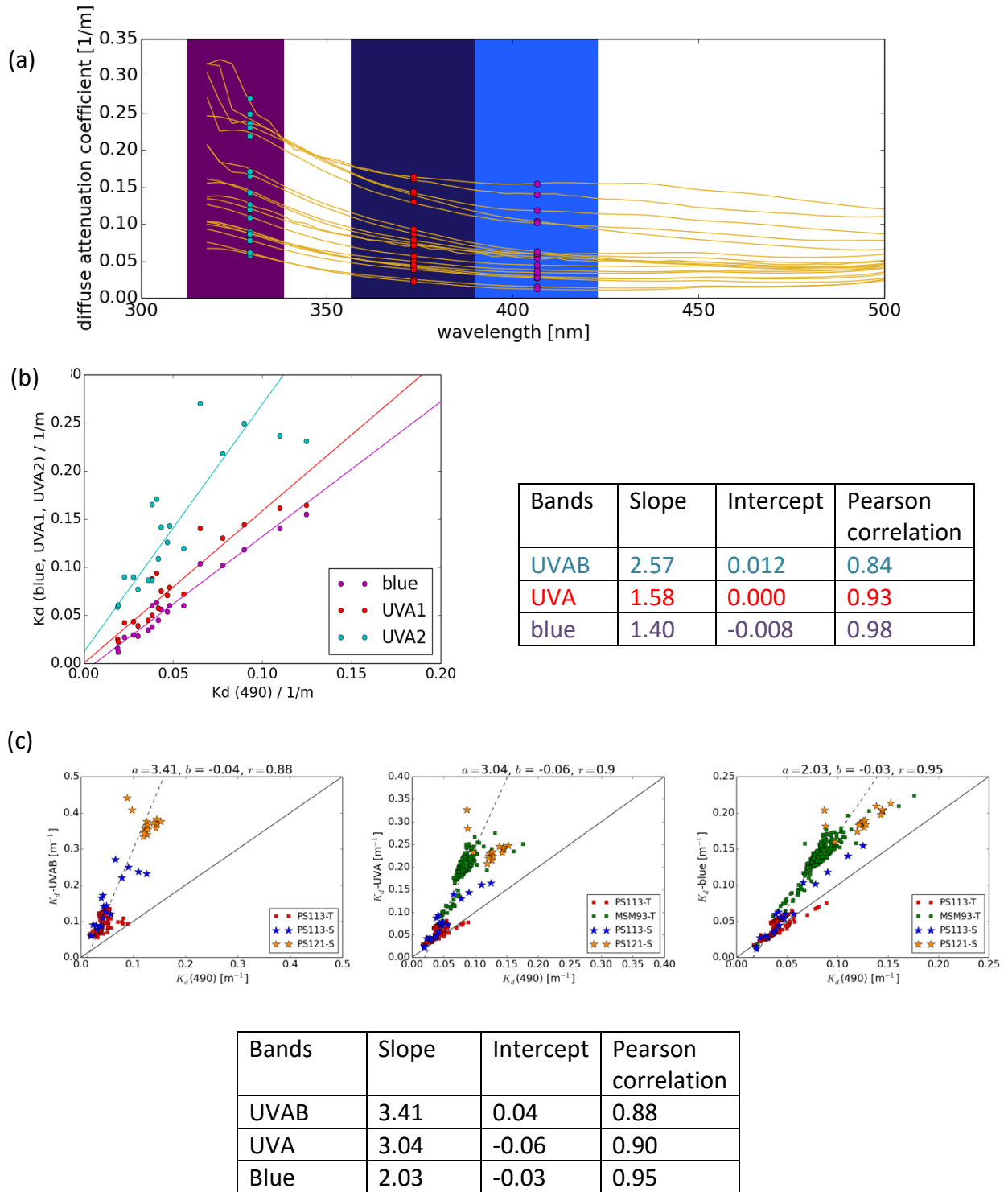
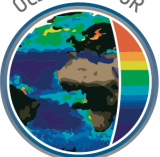



Figure 2:  $K_d$  spectral from RAMSES measurements (a) shown as background the wave band windows considered for S5POC TROPOMI  $K_d$  products (blue, UVA, UVAB); used to derive KD490 wavelength conversion to  $K_d$ -blue,  $K_d$ -

 <p><b>Exploitation of Sentinel-5-P for Ocean Colour Products (S5POC)</b></p>	<p>Validation Report</p>	<p>Ref: S5POC-PAL-VR Version: 1.0 Date: 20-12-2024 For: ESA and S&amp;T</p>
--	--------------------------	---

*UVA and  $K_d$ -UVAB shown as scatter plots and with parameters in table for (b) PS113 matchups only and (c) all available campaign data (region C and D, panel c).*

Statistical match-up analysis between S5POC TROPOMI  $K_d$  and RAMSES data from PS113 station data only and from regions C and D is presented in Table 3 and Figure 3. Match-ups between geolocation of PS113 and PS121 RAMSES stations (no RAMSES station data were available for MSM93) and TROPOMI ground pixels were calculated using a loose criterion given the low number of stations ( $N = 36$ ). We searched for each station for TROPOMI match-ups within  $\pm 2$  days and a radius of 5.5 km. If several match-ups were found in this time period, the 335 match-up closest in time to the satellite measurement is taken. If more than one TROPOMI pixel lies within search criteria, the mean TROPOMI  $K_d$  as calculated and the standard deviation was noted as uncertainty of the TROPOMI  $K_d$ . Using this loose criterion, match-ups were found for 9 stations. OLCI and OCCCI KD490 data were used to further quality control these 9 match-ups. The same spatial and temporal collocation criteria were applied to high-resolution OLCI data to find the corresponding OLCI data for each match-up. Following the Sentinel-3 ocean color validation protocol (EUMETSAT, 2021), OLCI match-ups were only considered valid if half of the pixel box was filled and if the coefficient of variation was not larger than 0.2. In addition, OCCCI match-ups were determined with spatial collocation criterion of 1 by 1 (corresponding to TROPOMI criterion) and 3 by 3 pixel box to additionally check the spatial homogeneity as for OLCI. 7 of the TROPOMI match-ups were confirmed to be valid for PS113 and only one for PS121 RAMSES station data. The same search criterion was applied to find match-ups between PS113 and MSM93 Triaxus RAMSES  $K_d$  data and TROPOMI  $K_d$  data. Again, matchups were searched with the same temporal and spatial window and match-ups closest in time to the satellite measurement were selected. TROPOMI  $K_d$  matchups were averaged in case more than one ground pixel lies within search radius. If several Triaxus measurements were matched with the same TROPOMI measurement, the Triaxus measurements were averaged and the standard deviation noted as variability in the Triaxus measurements, which indicates the spatial variability of the water mass. 37 match-ups remain after averaging. If several match-ups were found in this time period, the mean TROPOMI  $K_d$  was calculated from all match-ups per station. The standard deviation was noted as uncertainty of the TROPOMI  $K_d$ .

Table 3 contains statistical criteria of validation of TROPOMI  $K_d$  retrievals to in-situ data including bias, MAE, (unbiased)RMSD; some of this is further discussed in subsections 6.1.4 and 6.1.5. For all three waveband windows, the retrieved TROPOMI  $K_d$  significantly correlate with the observations ( $r > 0.5$  for PS113 stations only,  $r > 0.7$  for all, but UVA (0.4)). Figure 4 depicts the matchups geolocations between TROPOMI  $K_d$  and RAMSES PS113, PS121 and

 <p><b>Exploitation of Sentinel-5-P for Ocean Colour Products (S5POC)</b></p>	<p>Validation Report</p>	<p>Ref: S5POC-PAL-VR Version: 1.0 Date: 20-12-2024 For: ESA and S&amp;T</p>
--	--------------------------	---

MSM93.  $K_d$  measurements for the UVAB, UVA and blue bands. TROPOMI  $K_d$ -blue product reveals good performance especially for low  $K_d$ -blue (slope of 0.83 and 1.15 and an intercept of 0.01 and  $-0.02 \text{ m}^{-1}$ , respectively, for PS113 stations only). Considering the for PS113 station matchups vs. TROPOMI  $K_d$ -blue bias is much better than matchup statistics for S3-KD490 and OCCCI-KD490, and the same for intercept and bias, and slightly worse for  $r$ , MAE and RMSD ( $>0.64$ ,  $<0.009$  and  $<0.010$ , respectively, see Bracher et al., S3VT Meeting Dec 2020). TROPOMI  $K_d$ -UVAB is systematically lower (negative bias  $>0.023 \text{ m}^{-1}$  considering the small and the large matchup data set), while the slope is only much lower for the small data set (0.61). Compared to this for UVA, although the slope is higher for both data set ( $\sim 1.35$ ) the positive bias is much lower ( $\sim +0.011 \text{ m}^{-1}$ ). For TROPOMI  $K_d$  the bias, MAE, RMSD and unbiased are (much) lower for TROPOMI  $K_d$ -blue, and more similar for  $K_d$ -UVAB and  $K_d$ -UVA.

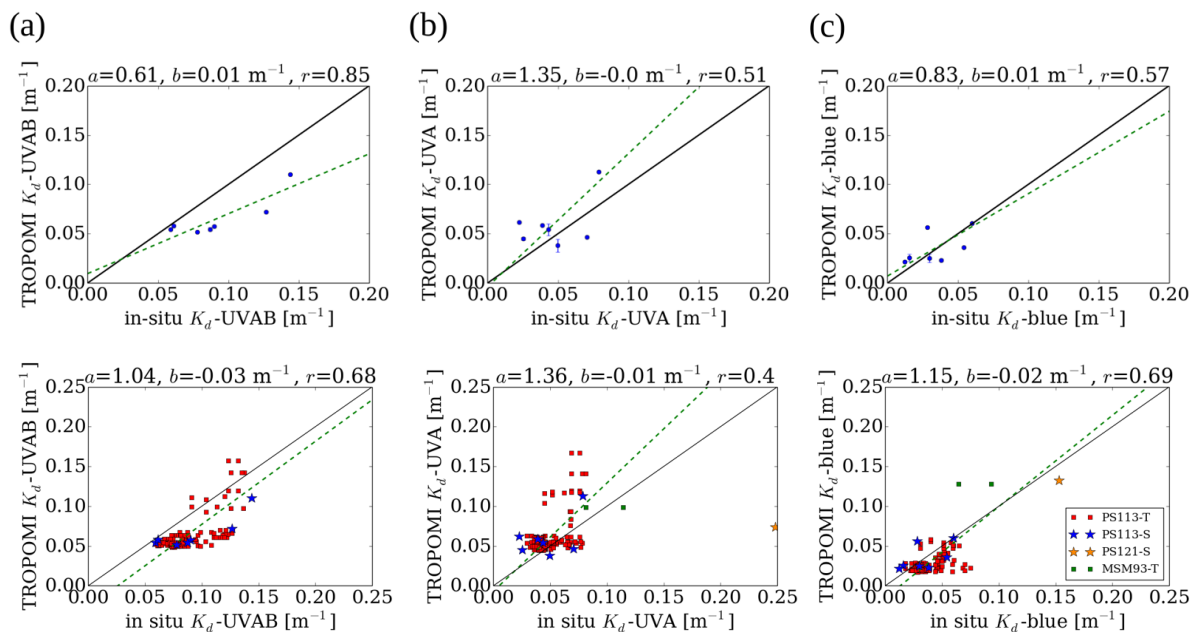



Figure 3:  $K_d$  -UVAB (A),  $K_d$  -UVA (B) and Kdblue (C) matchups (criterion  $\pm 2$  days, within radius 5.5 km) with RAMSES stations of PS113 (11 May – 9 June 2018,  $n=7$ ) and for all campaigns in regions C (PS113 stations  $n=7$  and Triaxus casts,  $n=35$ ) and D (PS121 stations ( $n=1$ ), MSM93 Triaxus casts ( $n=2$ , for UVAB no valid matchups)).

Table 3: S5POC TROPOMI  $K_d$  to in-situ spectral  $K_d$ , collected during PS113 stations only in the Atlantic Ocean (red,  $n=7$ ) and for all region C and D data (black,  $n=45$ ), matchup statistics

Criteria	KdUVAB	KdUVA	Kdblue
<b>R</b>	<b>0.85</b> 0.68	<b>0.51</b> 0.4	<b>0.57</b> 0.69

	<b>Exploitation of Sentinel-5-P for Ocean Colour Products (S5POC)</b>	<b>Validation Report</b>	Ref: S5POC-PAL-VR Version: 1.0 Date: 20-12-2024 For: ESA and S&T
---	---	--------------------------	---

<b>Bias (m<sup>-1</sup>)</b>	<b>-0.027</b> -0.023	<b>0.013</b> 0.011	<b>-0.002</b> -0.009
<b>MAE (m<sup>-1</sup>)</b>	<b>0.027</b> 0.025	<b>0.023</b> 0.018	<b>0.012</b> 0.013
<b>RMSD (m<sup>-1</sup>)</b>	<b>0.031</b> 0.029	<b>0.025</b> 0.028	<b>0.015</b> 0.016
<b>unbiased RMSD (m<sup>-1</sup>)</b>	<b>0.015</b> 0.018	<b>0.021</b> 0.026	<b>0.015</b> 0.016

The hyperspectral TROPOMI  $K_d$ -UVA and  $K_d$ -UVAB were only compared to TROPOMI  $K_d$ -blue (Table 4) and not to the multispectral data sets, since the wavelength conversion is less valid for the shorter wavelengths due to the different contribution of different sources of CDOM and UV absorbing pigments in different regions depending on the origin of water masses and productivity in the sea. The correlation between  $K_d$ -blue and  $K_d$ -UVA is lower than the one between  $K_d$ -blue and  $K_d$ -UVAB, the RMSD is similar and the MAE is larger for  $K_d$ -UVAB.

Table 4: Inter-comparison statistics for S5POC TROPOMI  $K_d$ -blue vs.  $K_d$ -UVA and  $K_d$ -UVAB as a full or masked (in brackets) data sets daily gridded 0.05° over the period of PS113 campaign.

Criteria	Kdblue vs. KdUVA	Kdblue vs. KdUVAB
R	0.44 (0.55)	0.53 (0.64)
Bias (m <sup>-1</sup> )	0.020 (0.019)	0.037 (0.039)
MAE (m <sup>-1</sup> )	0.039 (0.031)	0.051 (0.045)
RMSD (m <sup>-1</sup> )	0.073 (0.041)	0.071 (0.052)

For masked dataset, values above 0.3 m<sup>-1</sup> were excluded.

TROPOMI  $K_d$ -blue was intercompared to KD490 data from the multispectral OLCI (S3A L2) and OCCCI products. For the latter, KD490 was converted to  $K_d$ -blue via a linear wavelength conversion scheme. As seen in Figure 2 b and c, different wavelength conversion scheme seem appropriate for different regions due to the different composition of water constituents (high CDOM waters in the Arctic Ocean (region D, PS121 and MSM93) as opposed to the transatlantic waters (region C, PS113). Since not enough matchups were available for region D by itself, the wavelength conversion obtained from all matchups is used, while for the PS113 the station specific matchup conversion as in Oelker et al. 2022 was used. Since this

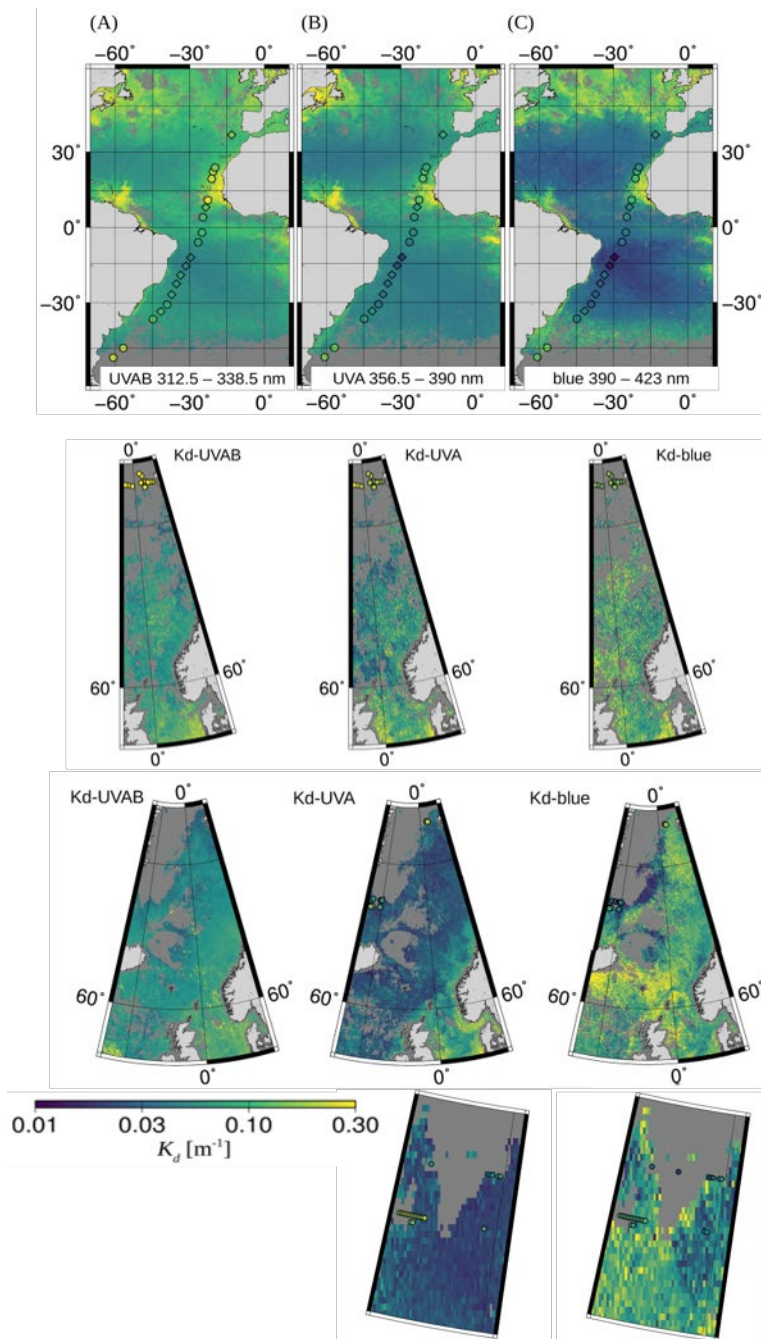



Figure 4: S5POC TROPOMI (A)  $K_d$ -UVAB, (B)  $K_d$ -UVA, and (C)  $K_d$ -blue gridded at  $0.083^\circ$  as mean for (upper panel) region C for the Atlantic Ocean for 11 May to 9 June 2018 (PS113 time period), (second upper panel) region D for the Transect from North Sea to the Arctic Ocean 11 Aug to 10 Sep 2019 (the PS121 time period), and (two lower panels) the East Greenland Sea 27 Jun to 25 Jul 2020 (time period MSM93, only  $K_d$ -UVA and  $K_d$ -UVA for detailed view  $70^\circ\text{N}$ - $75^\circ\text{N}$  and  $10^\circ\text{W}$ - $20^\circ\text{W}$ ). Accordingly,  $K_d$ -UVAB,  $K_d$ -UVA, and  $K_d$ -blue measured at stations during expedition PS113 and PS121 and at Triaxus casts during MSM93 are overlaid as diamonds (match-ups) and circles (unmatched stations).


 <p><b>Exploitation of Sentinel-5-P for Ocean Colour Products (S5POC)</b></p>	<p>Validation Report</p>	<p>Ref: S5POC-PAL-VR Version: 1.0 Date: 20-12-2024 For: ESA and S&amp;T</p>
--	--------------------------	---

wavelength conversion is principally valid for relating KD490 to  $K_d$ -blue, the comparison was restricted to  $K_d$ -blue and not extended to the  $K_d$ -UVAB and  $K_d$ -UVA. The evaluation of the S5POC TROPOMI  $K_d$ -blue against S3A  $K_d$ - and OCCCI  $K_d$ -blue is presented as matchups statistics (Figure 5 for conversion to KD490 and using triple collocation analysis, more details in sections 6.1.5 to 6.1.8, and Table 4 for Kdblue) based on daily products.

*Table 5: Intercomparison statistics for TROPOMI (S5P) vs. OCCCI and S3A  $K_d$ -blue as a full or masked (in brackets) data sets daily gridded  $0.05^\circ$  over the period of PS113 campaign (red) and for regions C for PS113, and for region and D for PS121 and MSM93 time periods (black). We define MAE as mean absolute deviation. For the masked dataset, values  $> 0.3 \text{ m}^{-1}$  for PS113 and  $> 0.5 \text{ m}^{-1}$  for all 3 campaigns and periods were excluded.*

Criteria	S5P vs. S3A	S5P vs. OCCCI	S3A vs. OCCCI
R	0.45 (0.77) 0.65 (0.72)	0.53 (0.74) 0.58 (0.71)	0.77 (0.87) 0.80 (0.86)
Bias ( $\text{m}^{-1}$ )	0.00 (0.00) -0.00 (0.00)	0.00 (-0.00) -0.01 (-0.00)	0.00 (0.00) -0.01 (-0.01)
MAE ( $\text{m}^{-1}$ )	0.03 (0.02) 0.03 (0.03)	0.02 (0.01) 0.03 (0.03)	0.02 (0.01) 0.02 (0.02)
RMSD ( $\text{m}^{-1}$ )	0.10 (0.03) 0.07 (0.05)	0.08 (0.03) 0.08 (0.05)	0.09 (0.02) 0.06 (0.03)
Unbiased RMSD ( $\text{m}^{-1}$ )	0.10 (0.03) 0.07 (0.05)	0.06 (0.03) 0.08 (0.05)	0.086 (0.017) 0.06 (0.03)

All above mentioned data sets were gridded to  $0.083^\circ$  on a daily basis for the study period. Significant correlation is found between S5POC TROPOMI  $K_d$ -blue and the multispectral  $K_d$ -blue, with slightly better agreement between S5POC and S3A (OLCI-A),  $r > 0.65$  and even  $r > 0.72$  for masked data set ( $K_d$ -blue  $< 0.5 \text{ m}^{-1}$ ), than between S5POC and OCCCI for the whole but similar for the masked data set ( $r = 0.71$ ). We note that the VRS fit factors underlying the  $K_d$ -blue product were corrected such that S5POC vs. OLCI yields a slope of one for an even smaller data set ( $K_d$ -blue  $< 0.15 \text{ m}^{-1}$ ) for the PS113 data set. For the larger masked data set ( $K_d$ -blue  $< 0.5 \text{ m}^{-1}$ ), a slope of unity is still found. Higher correlation is found between the multispectral data sets ( $r = 0.80$ ). The three products direct matchup comparison is further discussed in terms of bias and dispersion in subsections (6.1.4, 6.1.5).

	<b>Exploitation of Sentinel-5-P for Ocean Colour Products (S5POC)</b>	<b>Validation Report</b>	Ref: S5POC-PAL-VR Version: 1.0 Date: 20-12-2024 For: ESA and S&T
---	---	--------------------------	---

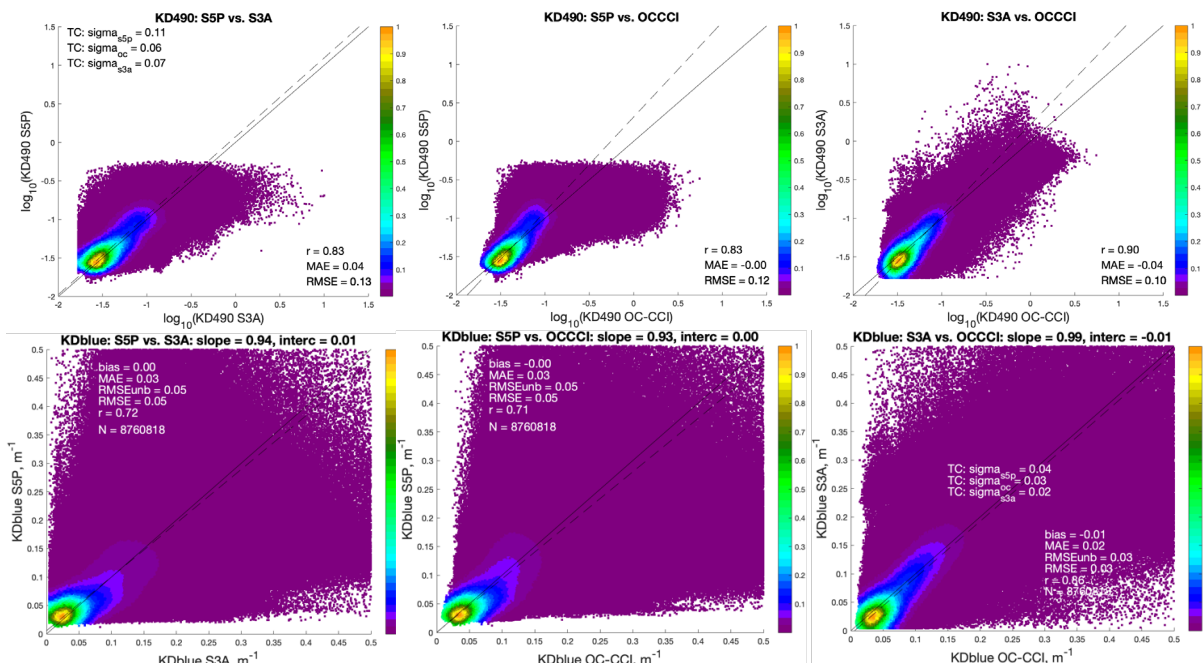
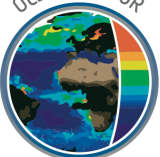


Figure 5: Matchups between (a) KD490 retrieved by S5POC TROPOMI and OCCCI, S5POC and S3A, and S3A and OCCCI in the Atlantic Ocean at the period of PS113 and (b)  $K_d$ -blue retrieved by S5POC and OCCCI, S5POC and S3A, and S3A and OCCCI for region C at the time period of PS113 and region D at the periods of PS121 and MSM93 together.

The S5POC TROPOMI  $K_d$ -blue product outperforms other hyperspectral  $K_d$ -blue products. The product quality is higher in more productive waters than for SCIAMACHY, OMI, and GOME-2. Oelker et al. (2019) limited the  $K_d$ -blue products from these three older hyperspectral sensors to below  $0.15 \text{ m}^{-1}$ . For these reduced data sets, correlations with OCCCI  $K_d$ -blue around 0.65 were achieved. Since their metrics are given for daily comparisons of almost one year of data, we cannot compare our monthly metrics one to one. However, S5POC TROPOMI  $K_d$ -blue correlation with the multispectral  $K_d$ -blue is above 0.65 and even above 0.7 for the masked data set including values up to  $0.5 \text{ m}^{-1}$ . The scatter plots presented in Oelker et al. (2019) show that the hyperspectral  $K_d$ -blue from SCIAMACHY and GOME-2 already diverge from the OCCCI  $K_d$ -blue in this range of the  $K_d$ -blue. Partially, this improvement is caused by the much lower ground pixel size of TROPOMI, which is closer to the multispectral satellite footprints, and thus reduces the representation error between the data sets. Smaller ground pixel sizes also reduce the inhomogeneity in satellite scenes improving fit quality. The improved DOAS fit quality of S5POC TROPOMI compared to its heritage sensors has also been found for UV-VIS retrievals of atmospheric trace gases (van Geffen et al., 2020; Seo et al., 2019).

 <p><b>Exploitation of Sentinel-5-P for Ocean Colour Products (S5POC)</b></p>	<p>Validation Report</p>	<p>Ref: S5POC-PAL-VR Version: 1.0 Date: 20-12-2024 For: ESA and S&amp;T</p>
--	--------------------------	---

The spread in the scatter plots appearing as a “butterfly shape” was first observed by Dinter et al. (2015) for SCIAMACHY and has appeared in all comparisons between hyper- and multispectral  $K_d$  products so far (see Figure 5 left and middle panel). A systematic difference in the method or sensor measurement technique seems to cause a behaviour where multispectral data see high  $K_d$  values for scenes for which the hyperspectral  $K_d$  is low and vice versa. Hardly any high  $K_d$  scenes occur in the data sets where hyper- and multispectral  $K_d$  are in agreement. This behaviour was discussed in Dinter et al. (2015) and Oelker et al. (2019) and attributed to low retrieval sensitivity for high  $K_d$ -values causing one wing of the distribution and to cloud contamination and large deviations from the average ocean scenario prescribed in the model causing the other wing.

### 6.3 Geographical pattern

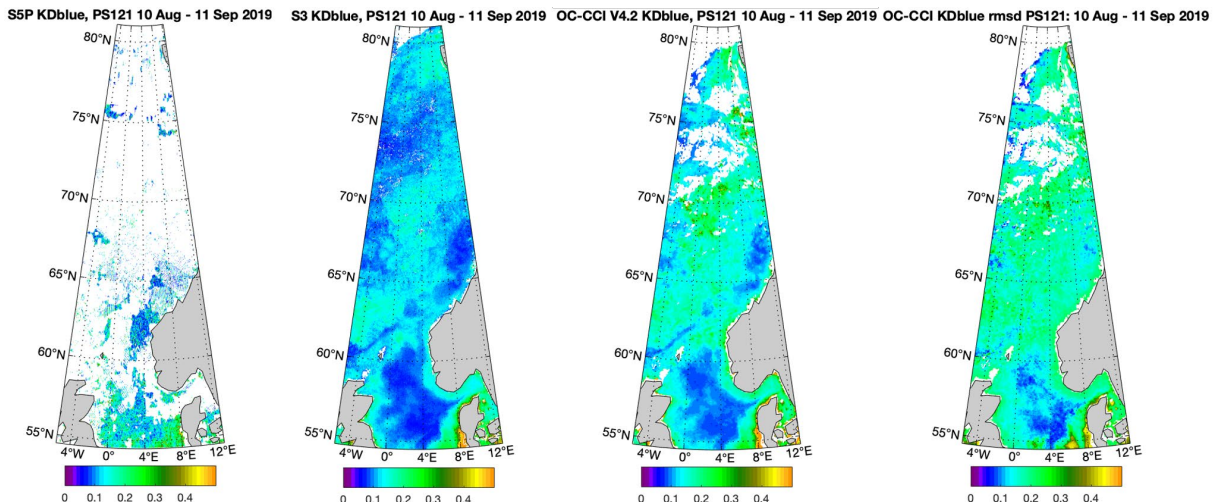
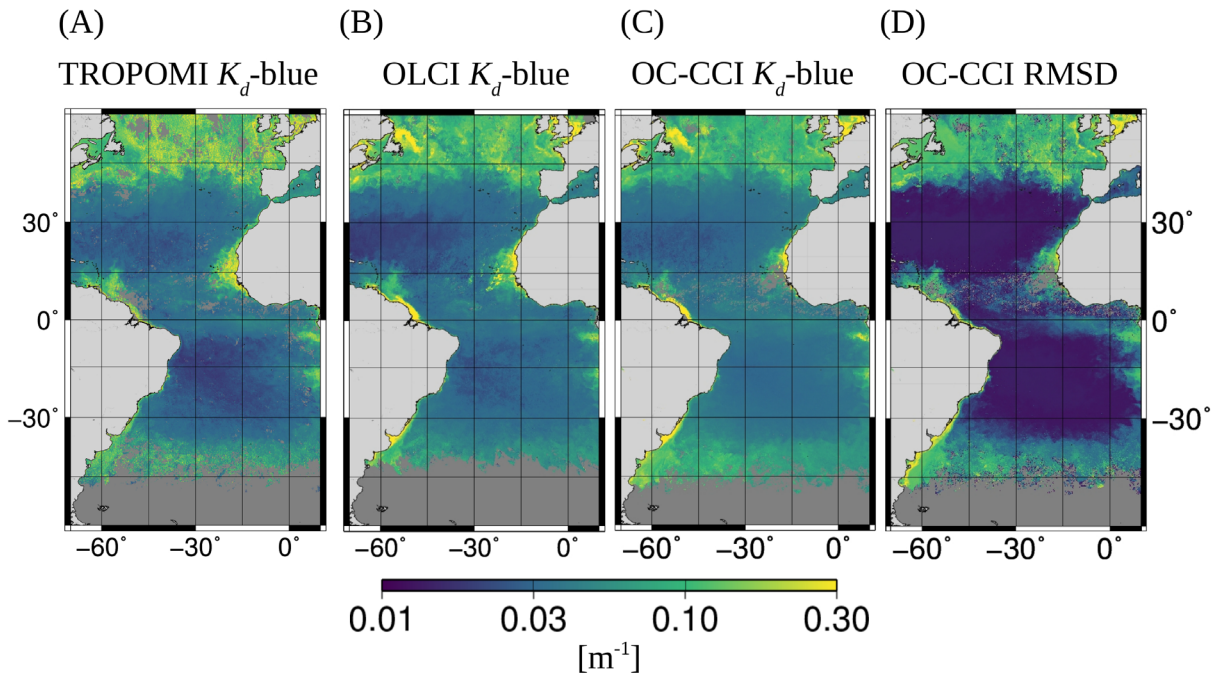
Figure 4 upper panel depicts  $K_d$  for three waveband windows: (A)  $K_d$ -UVAB, (B)  $K_d$ -UVA, and (C)  $K_d$ -blue in the Atlantic Ocean gridded to  $0.083^\circ$  and averaged over the time period of 11 May – 9 June 2018: Lowest  $K_d$  values are found in the North and South Atlantic Gyres, highest  $K_d$  in the upwelling regions along the African coast and the Amazon river plume. With decreasing wavelength,  $K_d$  increases. However,  $K_d$ -UVAB is not generally larger than  $K_d$ -UVA. In the upwelling regions off the coast of West African, the Amazon river plume, around Newfoundland, and around Great Britain the ratio  $K_d$ -UVA/  $K_d$ -UVAB is larger than 1.  $K_d$ -blue is strikingly larger than  $K_d$ -UVA and  $K_d$ -UVAB in the productive areas north of the Northern Atlantic Gyre.


In general, the S5POC TROPOMI  $K_d$ -values averaged over the PS113 time period agrees quite well the *in-situ* data values sampled at a specific time (Figure 4, depicted in circles or diamonds). However, S5POC TROPOMI  $K_d$  exceed those measured *in-situ* (e.g. in the South Atlantic Gyre). Exceptions are the two southernmost stations in the Malvinas upwelling region, where *in-situ*  $K_d$  is higher than the S5POC TROPOMI  $K_d$  for all three wavelength ranges. Though, satellite sampling is very sparse here and SZAs are large.

Unfortunately for region D, S5POC  $K_d$  data are sparse (three lower panels In Figure 4) due to the high solar zenith angle, especially for the late summer PS121 time period. However, we can still see that for the June-July typical phytoplankton blooming time period (MSM93, Figure 4 second lower panel) the Atlantic Waters in the Greenland are characterised by high  $K_d$ -blue values indicating phytoplankton blooms, opposed to the more western polar waters. The  $K_d$ -UVA values show no strong difference, indicating CDOM absorption not to be correlated to chl-a concentration.



Spatial patterns of the two S5POC TROPOMI  $K_d$ -UV products (Figure 4 two upper panels) are different. Daily comparisons of the gridded products with  $K_d$ -blue show a lower correlation



	<p><b>Exploitation of Sentinel-5-P for Ocean Colour Products (S5POC)</b></p>	<p>Validation Report</p>	<p>Ref: S5POC-PAL-VR Version: 1.0 Date: 20-12-2024 For: ESA and S&amp;T</p>
---	--	--------------------------	---

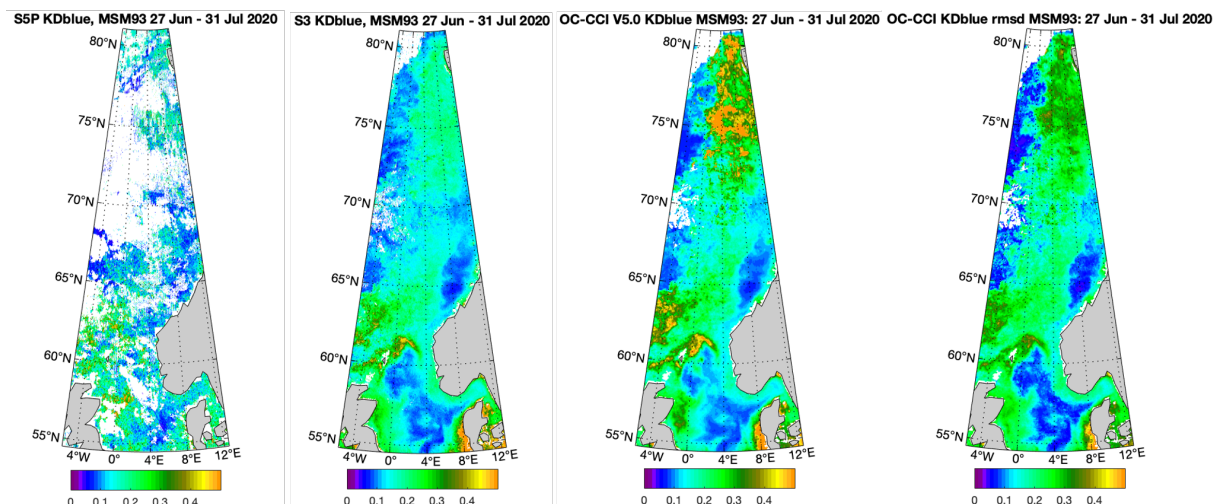



Figure 6: Spatial distribution of  $K_d$ -blue products from (A) S5POC, (B) S3A, (C) OCCCI, and (D) RMSD OCCCI gridded to  $0.083^\circ$  and averaged at the (upper panel) PS113 region and period 11 May – 9 June 2018, (middle panel) PS121 region and period 11 Aug to 10 Sep 2019, and (lower panel) MSM93 region and period 27 June to 25 July 2020. For S3A and OCCCI, the following conversion is used:  $K_d$ -blue =  $1.401 * KD490 - 0.0085$  for PS113 and  $K_d$ -blue =  $2.03 * KD490 - 0.03$  for PS121 and MSM93 is used, (d) RMSD as provided by OCCCI data set for the same grid and time periods.


with  $K_d$ -UVA than with  $K_d$ -UVAB. This observation contrasts the analysis of the spectral relationships between  $K_d$  at different wavelengths derived from the in-situ spectral  $K_d(\lambda)$ . However, we have to bear in mind that the quality of the in-situ measurements decreases with wavelength, naturally causing the correlation coefficient to decrease with wavelength. Other studies found also a decreasingly robust relationship with wavelength between  $K_d$  in the UV range and optical properties in the VIS range (Smyth, 2011; Johannessen et al., 2003; Vasilkov et al., 2005). A very robust relationship between  $K_d$  at 310 and 465 nm with correlation 0.998 was found in low-CDOM waters (Højerslev and Aas, 1991). It is therefore not generally clear, how robustly the  $K_d$ -UV are related to  $K_d$ -blue in different parts of the ocean. Light attenuation in the UV is mainly determined by CDOM and mycosporine-like amino acid (MAA) absorption. Based on its origin, CDOM has different absorption characteristics. VIS absorption is much stronger for humic substances with less steep spectral slope as opposed to mostly protein degrading substances of marine origin (Nelson and Siegel, 2002). MAA are UV-absorbing pigments of phytoplankton. Their production depends on UV irradiation and species composition (Vernet et al., 1994). MAA absorb between 320 and 350 nm with a peak around 330 to 340 nm (Vernet et al., 1994; Bracher and Wiencke, 2000). Presence of MAA should therefore mainly influence  $K_d$ -UVAB. Since the link between optical properties in different spectral regions of the UV-VIS is not robust from a biogeochemical perspective, it is necessary to directly infer spectral information on light penetration, highlighting the importance of this study. By covering three spectral regions, the TROPOMI  $K_d$ -products can give insight on CDOM

 <p><b>Exploitation of Sentinel-5-P for Ocean Colour Products (S5POC)</b></p>	<p>Validation Report</p>	<p>Ref: S5POC-PAL-VR Version: 1.0 Date: 20-12-2024 For: ESA and S&amp;T</p>
--	--------------------------	---

origin and MAA production. For the study period and on the same grid as in Figure 4, Figure 6 shows S5POC TROPOMI  $K_d$ -blue in comparison to S3A and OCCCI. Overall, S5POC TROPOMI  $K_d$ -blue patterns resemble the multispectral ones (e.g., gyres and productive areas around the Amazon river plume, Mauretanian upwelling system, English Channel, polar and Atlantic waters in the Greenland Sea). However, at latitudes  $>58^\circ$  for PS121 and  $>60^\circ$  for the MSM93 time period only few valid TROPOMI  $K_d$  pixels are available. This is because the TROPOMI  $K_d$  calculated via LUT is based on the coupled RTM SCIATRAN using the much faster non-spherical version which does not enable simulations at SZA  $>70^\circ$ . The S5POC TROPOMI  $K_d$ -blue product quality is especially similar in the clear water regions, but reduced in areas where TROPOMI  $K_d$ -blue  $> 0.3 \text{ m}^{-1}$ . Oelker et al. (2019) pointed out that the strength of the hyperspectral algorithm lies in low  $K_d$  waters since the VRS signal is highest here. The S5POC TROPOMI  $K_d$ -retrieval sensitivity decreases with increasing TROPOMI  $K_d$  (see discussion section 6.1.2). In some cases, the hyperspectral algorithm seems to fail for high TROPOMI  $K_d$  scenes causing obvious regional discrepancies, as in the waters around Newfoundland. Not only the general retrieval sensitivity plays a role for the performance in productive areas, also the model setup. Because we set up our RTM for case-I waters, our S5POC TROPOMI  $K_d$ -blue product is only valid for open ocean scenarios. For coastal applications, the RTM simulations have to be adjusted accordingly. The multispectral algorithms have already been adapted for high  $K_d$  waters. The semi-analytical algorithm by Lee et al. (2005b), used for the OCCCI product, has shown to perform well in coastal areas (Lee et al., 2005a) and inland waters (Gomes et al., 2018) whereas the OK2-555 algorithm by Morel et al. (2007b, used for the OLCI product, only covers case-1 waters.

#### 6.4 Bias


In comparison with matchup *in-situ* RAMSES PS113 (see Table 3), S5POC TROPOMI  $K_d$  data show low bias for the blue wavelength window ( $\text{bias}_{K_d\text{-blue}} = -0.004 \text{ m}^{-1}$ ) and bias of a similar range for UV ( $\text{bias}_{K_d\text{-UVA}} = -0.035 \text{ m}^{-1}$ ;  $\text{bias}_{K_d\text{-UVAB}} = -0.039 \text{ m}^{-1}$ ). It is noticeable that S5POC  $K_d$ -UVAB is systematically higher than the *in-situ*  $K_d$ -UVAB over the sampled  $K_d$  range (Figure 4a). In this respect, it is worth mentioning that quality of the *in-situ*  $K_d$  at short wavelengths is limited. The TriOS sensor only measures down to 320 nm and its measurement accuracy appears to decrease towards this lower end of the spectral range as observed also by other users (Nicolaus et al., 2010). Consequently, the *in-situ*  $K_d$ -UVAB has a spectral mismatch to the TROPOMI  $K_d$ -UVAB. Evaluated from the RTM simulations, a 5 to 10% higher satellite  $K_d$ -UVAB could be expected, restrictedly explaining the bias we found for S5POC TROPOMI  $K_d$ -UVAB from the match-up analysis. The S5POC TROPOMI  $K_d$  product seems to have a small multiplicative bias, which is not only apparent from the *in-situ* data comparison, but also from calculating the ratio between S5POC TROPOMI  $K_d$ -UVA and -UVAB, which is larger than 1 for

 <p><b>Exploitation of Sentinel-5-P for Ocean Colour Products (S5POC)</b></p>	<p>Validation Report</p>	<p>Ref: S5POC-PAL-VR Version: 1.0 Date: 20-12-2024 For: ESA and S&amp;T</p>
--	--------------------------	---

high  $K_d$  waters.  $K_d$ -UVAB should always be larger than  $K_d$ -UVA from a theoretical point of view considering that CDOM absorption decreases exponentially with wavelength.

A decreasing  $K_d$  with decreasing wavelength in the UV is backed up by field data (Baker and Smith, 1982; Conde et al., 2000). An exception might be waters with extremely low CDOM concentrations for which hardly any difference was observed between  $K_d$  at 310 and 465 nm (Højerslev and Aas, 1991). The multiplicative bias might be correctable by adding an offset to the VRS fit factors in the short blue fit window similar to the offset correction performed for  $K_d$ -blue. We did not try to correct the VRS fit factors used to calculate  $K_d$ -UVA, since the wavelength conversion is less robust and no reference data set is available at the moment. The multiplicative bias becomes important in CDOM-rich or productive areas in the open ocean. For  $KD < 0.3\text{m}^{-1}$ , covering large parts of the open ocean,  $K_d$ -UVA is a robust estimator for UVA light penetration as concluded from the *in-situ* comparison (see section 6.1.2 discussion).

On PS113 basin-averaged, in comparison with S3A and OCCCI KD products, the bias of S5POC TROPOMI  $K_d$ -blue is low (0 – 4%) (direct daily matchups in Figure 5 and Table 4), while there are regional differences between TROPOMI and the multispectral  $K_d$ -blue (Figure 7; based on daily matchups): north of Newfoundland OLCI and OCCCI show similar high-KD patterns whereas this pattern does not occur in the S5POC TROPOMI  $K_d$ -blue product; around Great Britain,  $K_d$ -blue patterns from the multispectral products are not so similar to each other as those from OCCCI compared to S5POC; in the Subtropical Gyre, S5POC TROPOMI  $K_d$ -blue is lower than those from OCCCI (to a larger extent in the Southern Hemisphere), but nevertheless higher than S3A product in the northern Subpolar Gyre. Other regional differences appear in the Mauretanian and Malvinas upwelling systems.

 <p><b>Exploitation of Sentinel-5-P for Ocean Colour Products (S5POC)</b></p>	<p>Validation Report</p>	<p>Ref: S5POC-PAL-VR Version: 1.0 Date: 20-12-2024 For: ESA and S&amp;T</p>
--	--------------------------	---

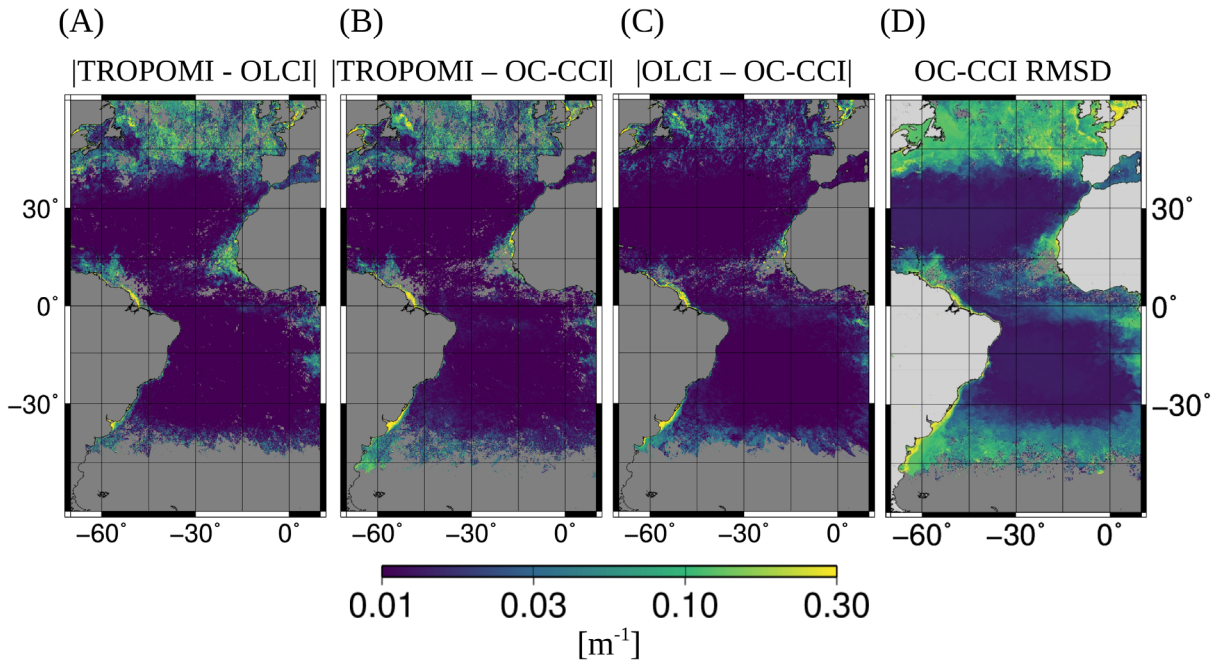



Figure 7: Mean absolute difference between (A) S5POC TROPOMI and OLCI, (B) S5POC TROPOMI and OLCI, and (C) OLCI and OLCI  $K_d$ -blue for the time period 11 May to 9 June and gridded at  $0.083^\circ$ . (D) RMSD as provided in OLCI data set for same grid and time period.

### 6.5 Dispersion

As a statistical measure of the dispersion between S5POC TROPOMI  $K_d$  and in-situ spectral  $K_d$  observations, Table 3 presents the unbiased RMSD of S5POC TROPOMI  $K_d$  from in-situ PS113 measurements: The performance of TROPOMI  $K_d$ -blue and  $K_d$ -UVAB is similar ( $0.017 \text{ m}^{-1}$ ) and worse for  $K_d$ -UVA ( $0.031 \text{ m}^{-1}$ ).

Table 4 contains unbiased RMSD of  $K_d$ -blue from S3A and OLCI  $K_d$ -blue (after converting from standard KD490 products) as compared to each other and to S5POC TROPOMI  $K_d$ -blue. These estimates are provided for the full collocated matchups dataset and a masked (reduced) data set excluding values higher than  $0.3 \text{ m}^{-1}$ . As a motivation, for considering the masked data set, is the obtained Gaussian distribution for  $K_d$ -blue which is not the case for the full dataset (Oelker et al. 2020); therefore, this makes the applicability of such a statistical criterium as RMSD (as well as Pearson correlation coefficient) questionable. Again, we can point here to discussion of the spread in the related scatter plots, presented in Figure 5, and discussion on this presented in section 6.1.2: The systematic difference in the algorithm and/or sensor measurement technique seems to cause a behavior where multispectral data see high  $K_d$  values for scenes for which the hyperspectral  $K_d$  is low and vice versa. Hardly any high  $K_d$  values occur in the data sets where hyper- and multispectral KD are in agreement. Further as discussed in Dinter et al. (2015) and Oelker et al. (2019), besides the attribution of the retrieval

 <p><b>Exploitation of Sentinel-5-P for Ocean Colour Products (S5POC)</b></p>	<p>Validation Report</p>	<p>Ref: S5POC-PAL-VR Version: 1.0 Date: 20-12-2024 For: ESA and S&amp;T</p>
--	--------------------------	---


sensitivity causing one wing of the distribution and cloud contamination and large deviations from the average ocean scenario prescribed in the RTM simulations probably are causing the other wing (Oelker et al. 2020). For the reduced data set the dispersions between S5POC TROPOMI  $K_d$ -blue and both multispectral S3A and OCCCI  $K_d$ -blue data are similar ( $unbiasedRMSD = 0.027 m^{-1}$ ), while S3A and OCCCI  $K_d$ -blue data products slightly in better agreement to each other ( $unbiasedRMSD = 0.017 m^{-1}$ ). A similar conclusion can be drawn from MAE(D) estimates presented in Table 2, which are  $0.015 m^{-1}$ ,  $0.015 m^{-1}$  and  $0.09 m^{-1}$  for S5POC vs. S3A, S5POC vs. OCCCI and S3A vs. OCCCI, respectively.

Table 6: Statistics on S5POC vs. OCCCI and S3A log-transformed  $K_d$ -blue evaluation based on spatial distribution of data composites (gridded to  $0.025^\circ$ ) over the period of PS113 campaign.

Criteria	S5P vs. S3A	S5P vs. OCCCI	S3A vs. OCCCI
R	0.83	0.83	0.90
Bias	0.04	0.00	-0.04
RMSD	0.13	0.12	0.10

Bias and RMSD are provided for log-transformed  $K_d$  values and could be considered as relative errors.

To tackle the problem of non-Gaussianity distribution of the full dataset, a statistical analysis was performed for log-transformed S5POC, S3A and OCCCI  $K_d$ -blue. Table 6 presents RMSD calculated based on spatial distribution of log-transformed data composites (gridded to  $0.025^\circ$ ) over the period of PS113 campaign. Figure 7 depicts related matchups with a frequency distribution on the background. As seen, the S5POC  $K_d$ -blue agrees with multispectral S3A and OCCCI data with RMSDs equal to 0.13 and 0.12 respectively. The RMSD of S3A  $K_d$ -blue from OCCCI  $K_d$ -blue is a bit smaller ( $RMSD = 0.10$ ). Again, the agreement between the two multispectral  $K_d$  data sets is a bit higher than between multi- and hyperspectral. Similar conclusion can be drawn from estimated MAD (Table 4). Partially, this discrepancy may be explained by the uncertainty associated with the wavelength conversion, but there could be other reasons why the multispectral products are in better agreement. Although the products are obtained from different algorithms and different multispectral satellite sensors, the measurement principle of the sensors is the same for these data sets, e.g., both starting with water leaving reflectance as input data, while S5POC uses TOA radiances from TROPOMI as input. In addition, ocean color sensors are designed for this application and have a higher signal-to-noise ratio than TROPOMI for ocean scenes. The S5POC TROPOMI  $K_d$ - products are naturally a bit noisier, also due to larger ground pixel sizes.

 <p><b>Exploitation of Sentinel-5-P for Ocean Colour Products (S5POC)</b></p>	<p>Validation Report</p>	<p>Ref: S5POC-PAL-VR Version: 1.0 Date: 20-12-2024 For: ESA and S&amp;T</p>
--	--------------------------	---

Additionally, to estimate the variance of the S5POC  $K_d$ -blue(KD490) in a context of comparison with available multispectral satellite  $K_d$  data products, we performed the triple collocation (TC) analysis (details in RD3). Figures 8 and 9 depict results of TC analysis (RD3) of the developed S5POC TROPOMI  $K_d$ -blue/KD490 products and similar products derived from multispectral S3A and OCCI data for the same period as PS113. Prior to the TC analysis all three data products were projected to a grid with  $0.025^\circ$  resolution. As seen, S5POC TROPOMI  $K_d$ -blue/490 reveals higher deviation at Northern temperate latitudes ( $>40^\circ\text{N}$ ) in comparison with other two  $K_d$ -products and with S5POC TROPOMI  $K_d$ -product deviation in subtropical regions.

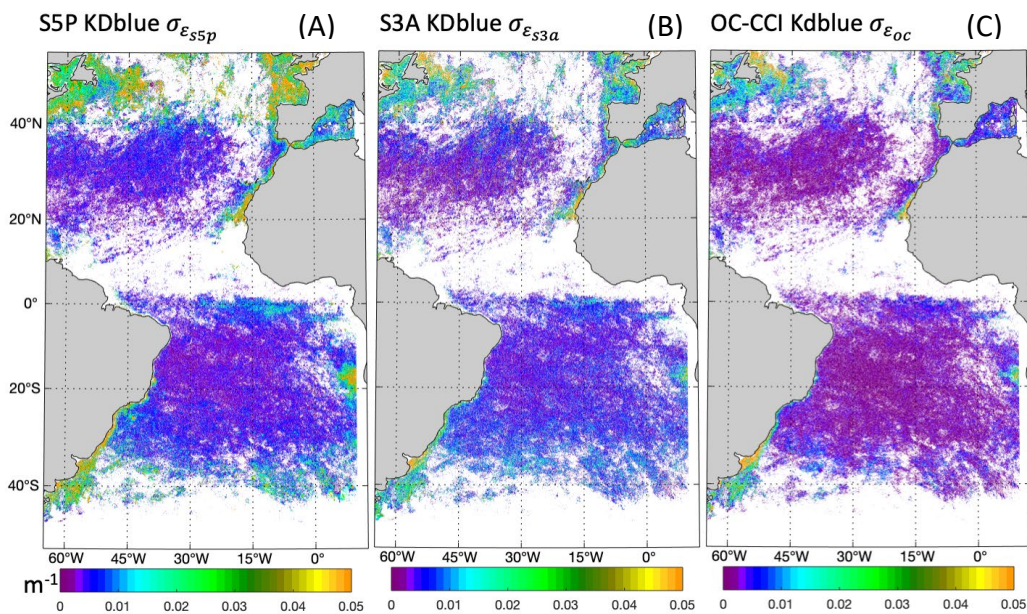


Figure 8: Dispersion of  $K_d$ -blue (KDbblue) estimates ( $m^{-1}$ ) obtained for S5P, S3A and OCCI over the period of PS113 campaign. The statistics is derived based on TC analysis. For S3A and OCCI, the following conversion is used:  $K_d$ -blue =  $1.401 * KD490 - 0.0085$  (RD3).

Generally, the spatial distribution of the obtained uncertainties is consistent with the above discussed differences between the satellite products. However, north of Newfoundland both multispectral S3A (OLCI) and OCCI show higher than S5POC TROPOMI TC-base uncertainties. It is also worth mentioning that the obtained S5POC TROPOMI  $K_d$ -values uncertainties are within (less than) OCCI data errors (Figure 10). It is worth mentioning that the TC analysis relates to the variability explained by all three data products. It could be that one of the products underestimates the true variability. For instance, OCCI KD490 is underestimated in the subtropical gyres (Figure 10), which results in low TC uncertainties for this product.

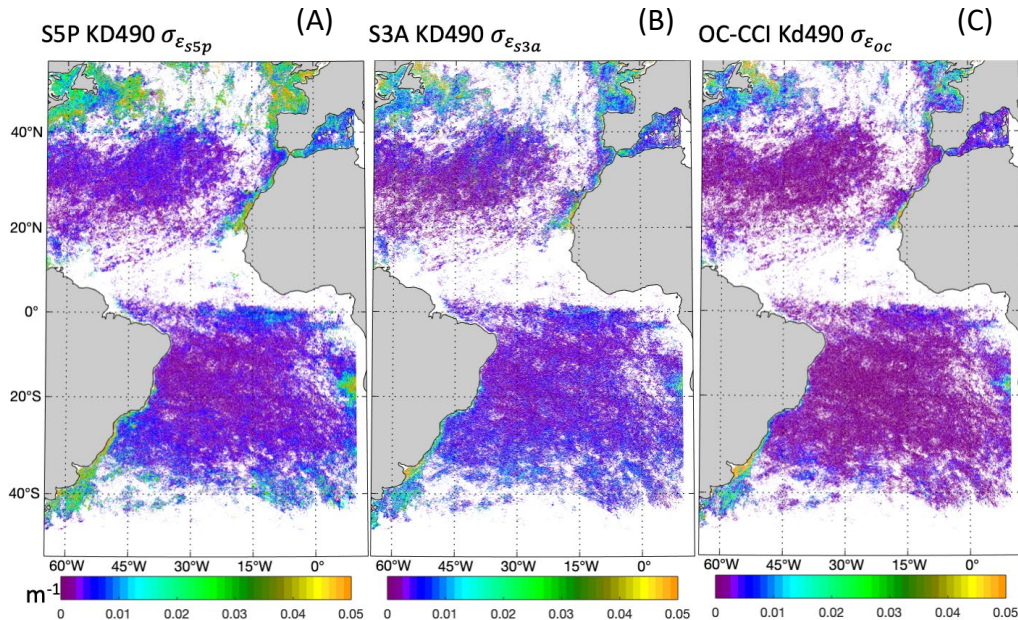



Figure 9: Dispersion of KD490 estimates ( $m^{-1}$ ) obtained for S5P, S3A and OC-CCI over the period of PS113 campaign. The statistics is derived based on TC analysis. For S5POC product the following conversion is used:  $KD490 = (K_d\text{-blue} + 0.0085)/1.401$  (RD3).

In summary, the reported above higher agreement between the two multispectral Kdblue data sets than between multi- and hyperspectral ones (Figure 7, Tables 4 and 6) has to be put into perspective, considering different ground pixel sizes of the sensors. In addition, a perfect correlation between multi- and hyperspectral products is not expected due to the uncertainty associated with the wavelength conversion. We therefore want to stress the importance of direct retrievals of KD at other wavelengths. However, we are confident that the comparison between the hyperspectral and multispectral  $K_d\text{-blue}$  is robust in the oligotrophic waters of our study area because wavelength conversion was calculated from in-situ data measured in exactly these waters in the time period of the PS113.



	<b>Exploitation of Sentinel-5-P for Ocean Colour Products (S5POC)</b>	<b>Validation Report</b>	Ref: S5POC-PAL-VR Version: 1.0 Date: 20-12-2024 For: ESA and S&T
---	---	--------------------------	---

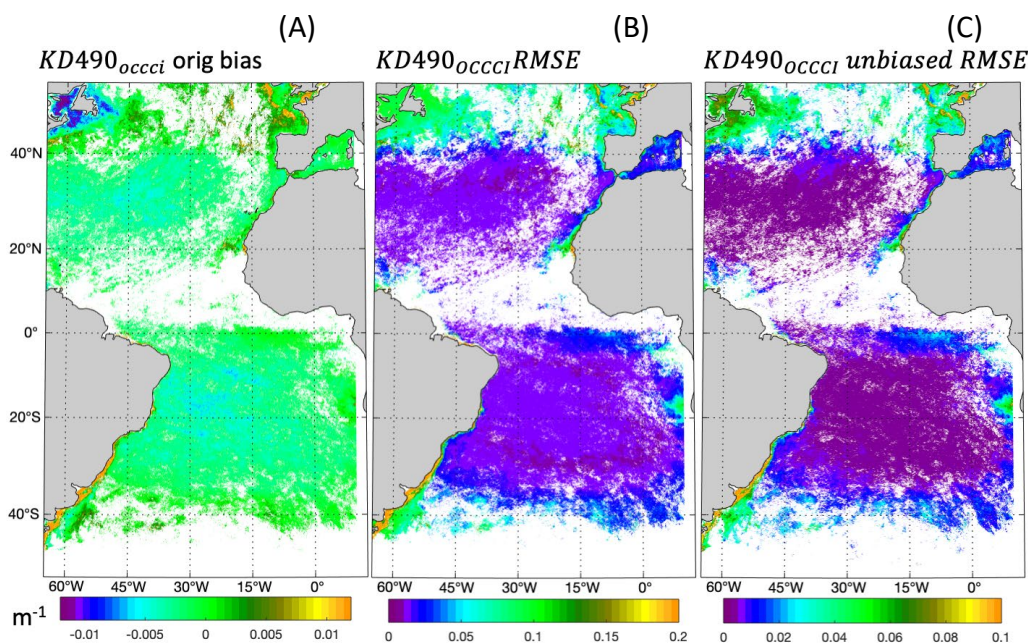


Figure 10: PS113 composites of original bias, RMSE and unbiased RMSE of  $KD490$  ( $m^{-1}$ ) provided by OCCCI. (The composites are based on collocations of updated S5POC KD with those from S3A and OCCCI) The error statistics is provided for  $KD490$  and are to be multiplied by 1.401 to converted to the blue range.

## 6.6 Short term variability

All the presented above S5POC TROPOMI  $K_d$ -blue, -UVA and -UVAB evaluation against *in-situ* KD spectral measurements and multispectral S3A and OCCCI KD data products were carried out over one month period (11 May – 10 June 2018) for region C. In general, this new TROPOMI data product agrees well with the considered *in-situ* and satellite observations. However, it is difficult to make any conclusion on the S5POC TROPOMI  $K_d$ -product quality with respect to capturing the variability observed within this (a short) PS113 time period. The TC analysis (given the number of collocations of all three data products) of the  $K_d$ -blue products shows, that over this period of time, temporal variability of a true signal is much lower than the differences between the products or product dispersions around the truth. This is clearly seen from the spatial distribution of fractional mean-squared-error (fMSE, see RD3) depicted in Figure 11: The fMSE for all three data products are close to 1 at low-to-mid latitudes, which indicates very low variability of the true signal/observed quantity over the considered 1 month time period. Only at latitudes higher than 40°, a true signal could be detected and correlation of the considered  $K_d$ -blue products to the true signal could be found (visualized in Figure 12).

Thus, the correlation between S5POC TROPOMI  $K_d$  and in-situ and multispectral  $K_d$  information discussed in previous subsections relates mostly to similarity in spatial distribution of the considered observations.

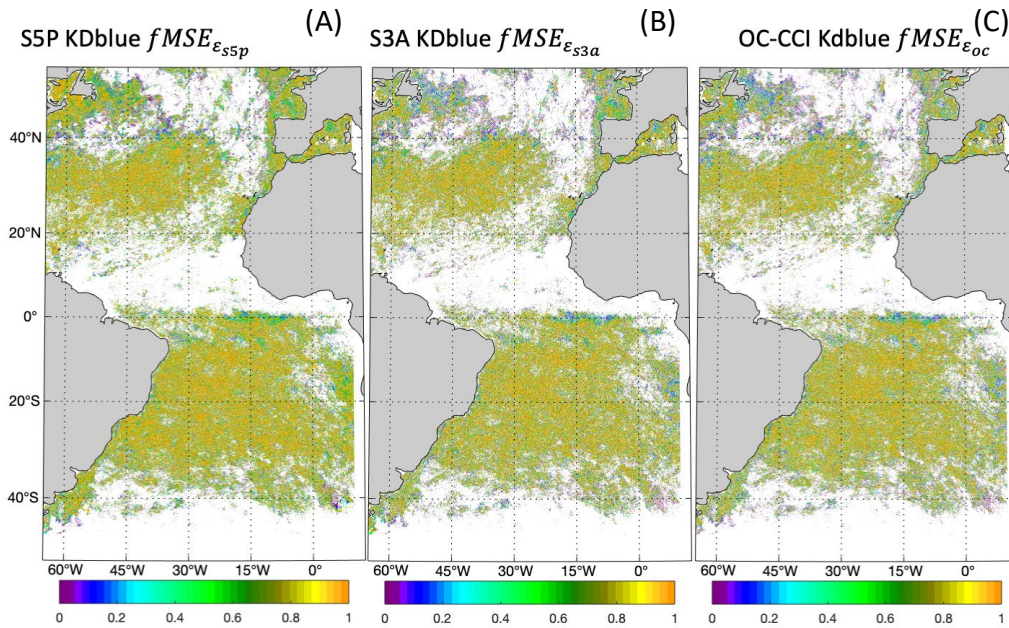
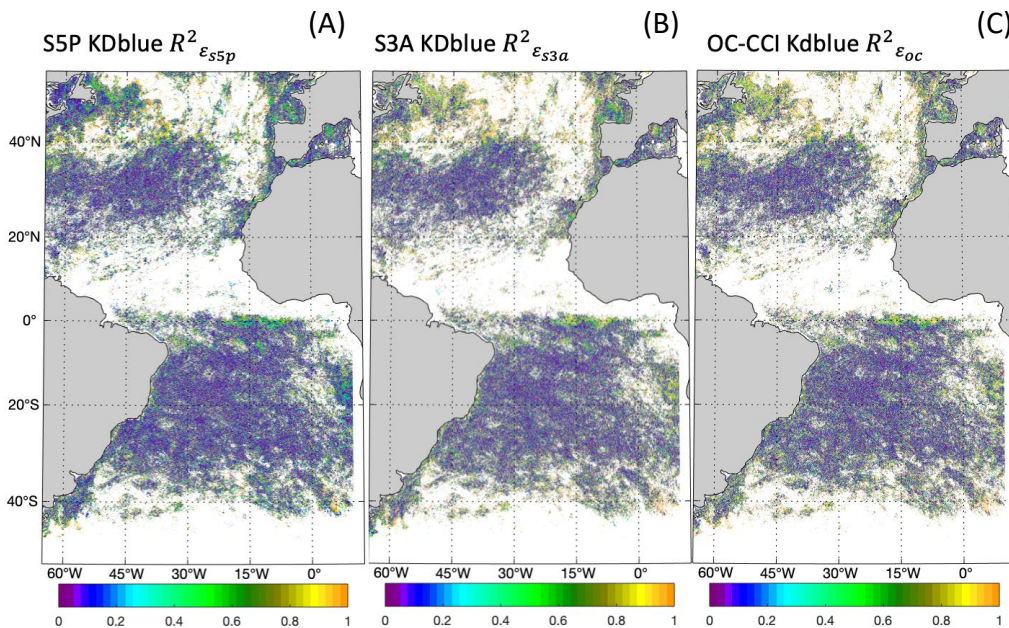


Figure 11: Fractional mean squared deviation of log-transformed  $K_d$ -blue estimates obtained for S5P, S3A and OCCI from the “truth” explained by all three products over the period of PS113 campaign. The statistics is derived based on TC analysis. For S3A and OCCI, the following conversion is used:  $K_d$ -blue =  $1.401 * KD490 - 0.0085$  (RD3).



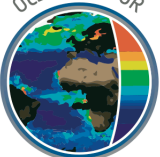

 <p><b>Exploitation of Sentinel-5-P for Ocean Colour Products (S5POC)</b></p>	<p>Validation Report</p>	<p>Ref: S5POC-PAL-VR Version: 1.0 Date: 20-12-2024 For: ESA and S&amp;T</p>
--	--------------------------	---

Figure 12: Correlation of log-transformed  $K_d$ -blue estimates obtained for S5P, S3A and OCCCI to the “truth” explained by all the tree products over the period of PS113 campaign. The statistics is derived based on TC analysis. For S3A and OCCCI, the following conversion is used:  $K_d$ -blue =  $1.401 \cdot KD490 - 0.0085$  (RD3).

## 6.7 Dependence on influence quantities

In contrast to TROPOMI, a north-south trend was observed for the Gyres for OCCCI and OLCI  $K_d$ -blue with lower values in the Northern than in the Southern Gyre. A similar trend as for TROPOMI  $K_d$ -blue was observed for SCIAMACHY and OMI (Oelker et al., 2019). While in case of SCIAMACHY the latitudinal trend was attributed to polarization effects, the SZA angle dependence of OMI VRS retrievals did not match the SZA dependence as predicted by the model. From our experience with building the 3-dimensional LUT for TROPOMI, additionally including the VZA, we conclude that also for TROPOMI the SZA and VZA dependence of theoretical VRS fit factors as predicted by the RTM is not aligned with that of satellite retrieved VRS fit factors. Since angular dependencies are largely controlled by surface roughness, it might be worthwhile to extend the LUT with wind speed as an input parameter available from climatologies. However, the false angular dependency might also be a DOAS-retrieval related problem, e.g., caused by an angle-dependent correlation with  $O_4$ .

In addition, the case I assumption used in the simulations is generally not valid in the UV domain. The absorption coefficient cannot be accurately described using Chla (Morel et al., 2007a; Vasilkov et al., 2001). The influence of RTM settings on the three  $K_d$ -retrievals was therefore investigated (section 7.2 in [RD3]) which is summarized here: Case-I parameterization for the visible wavelength range were used in combination with a recent pure water absorption spectrum accurately measured for UV wavelengths (Mason et al., 2016). Highest uncertainty lies within the settings for phytoplankton and CDOM absorption. Presence of MAA causes higher UV absorption than prescribed in our standard case-I parameterization. High variability can also be expected for the CDOM slope (Vodacek and Blough, 1997), considering its variation from 0.01 to 0.03  $\text{nm}^{-1}$ , as compared to the constant value of 0.014  $\text{nm}^{-1}$  used in the standard case-I scenario. Therefore, the PhytoDOAS retrievals' sensitivity was investigated by RTM already for  $K_d$ -blue in Oelker et al. (2019) and now for  $K_d$ -UV within S5POC (Oelker et al. 2022, [RD3]). The investigated influence of aerosol and magnitude of the CDOM absorption on the  $K_d$ -blue retrieval showed overall low significance. Using a much lower CDOM slope (0.007  $\text{nm}^{-1}$ ) than in the RTM setting for this TROPOMI retrieval leads to an overestimation of  $K_d$ -UVAB between 0 and 20%, a higher CDOM slope (0.03  $\text{nm}^{-1}$ ) to an underestimation between 10 and 30% in the range  $K_d$ -UVAB  $< 0.3 \text{ m}^{-1}$  (roughly 8% lower over- and underestimation for  $K_d$ -UVA), as well as an underestimation of up to 20%,

 <p><b>Exploitation of Sentinel-5-P for Ocean Colour Products (S5POC)</b></p>	<p>Validation Report</p>	<p>Ref: S5POC-PAL-VR Version: 1.0 Date: 20-12-2024 For: ESA and S&amp;T</p>
--	--------------------------	---

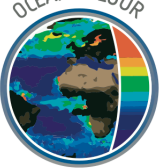
when an absorption spectrum with medium MAA absorption is used (S9 from Bracher and Wiencke, 2000). Considering the high variability in optical properties that can be expected for the UV range (see Figure 18 in [RD3]) and the difficulty to parameterize it, the S5POC TROPOMI  $K_d$ -UV retrievals are only moderately sensitive to the chosen parameterization. Changes in  $K_d$ -UV caused by changes in CDOM and phytoplankton absorption should therefore be resolvable.

## 7 Conclusions

We successfully exploited S5P's sensor TROPOMI's UV-VIS bands for deriving diffuse attenuation,  $K_d$ , in the open ocean. This first application of TROPOMI data for oceanic retrievals gave plausible results for three  $K_d$  products (Oelker et al. 2022, Oelker 2021). Two novel  $K_d$  products in the UV (312.5 to 338.5 nm (UVAB) and 356.5 to 390 nm (UVA)) were presented showing robust agreement with  $K_d$  *in-situ* data. In addition, a  $K_d$  product in the blue was retrieved (390 to 423 nm) that showed a better performance than  $K_d$ -blue from SCIAMACHY, GOME-2 and OMI in earlier studies.  $K_d$ -blue agrees well with the wavelength-converted KD490 products from the multispectral data sets OLCI and OCCCI. The multispectral data sets have a slightly better agreement amongst each other than with the hyperspectral data set. However, differences between the three  $K_d$ -blue products were found to be within the uncertainties of the OCCCI data set.

The robust agreement of S5POC TROPOMI  $K_d$  products with *in-situ* and multispectral data sets shows that VRS can be successfully retrieved using PhytoDOAS and converted to  $K_d$  using an RTM-based LUT. However, we identified a few retrieval issues which could be investigated in more detail and made suggestions for improving the LUT in the future. A major issue was an offset correction that had to be applied to the VRS fit factors going into the  $K_d$ -dblue product. The S5POC Kdblue product is therefore not independent. A correlation with  $O_4$  was found that might cause this offset. Finding a correction that aims at the origin of this problem and is independent from other  $K_d$  data sets is desirable (Oelker et al. 2022).

So far, S5POC TROPOMI  $K_d$  products for scenes with  $K_d > 0.5 \text{ m}^{-1}$  should be treated with caution. Unfortunately, not all open ocean scenes can be covered with the presented S5POC TROPOMI  $K_d$  data set, since higher  $K_d$  values are typically found for, e.g., spring blooms in the high latitudes. However, valuable information can be drawn in large parts of the open ocean. In clear water regions, the S5POC TROPOMI  $K_d$  products might even outperform the multispectral  $K_d$  products from a theoretical point of view. Extensive comparisons with *in-situ* data are necessary to answer this question. As a next step, a  $K_d$  time series over the TROPOMI

 <p><b>Exploitation of Sentinel-5-P for Ocean Colour Products (S5POC)</b></p>	<p>Validation Report</p>	<p>Ref: S5POC-PAL-VR Version: 1.0 Date: 20-12-2024 For: ESA and S&amp;T</p>
--	--------------------------	---

recording time period can be derived and analyzed on global scales to investigate temporal and spatial stability of the products.

----- END OF THE DOCUMENT -----